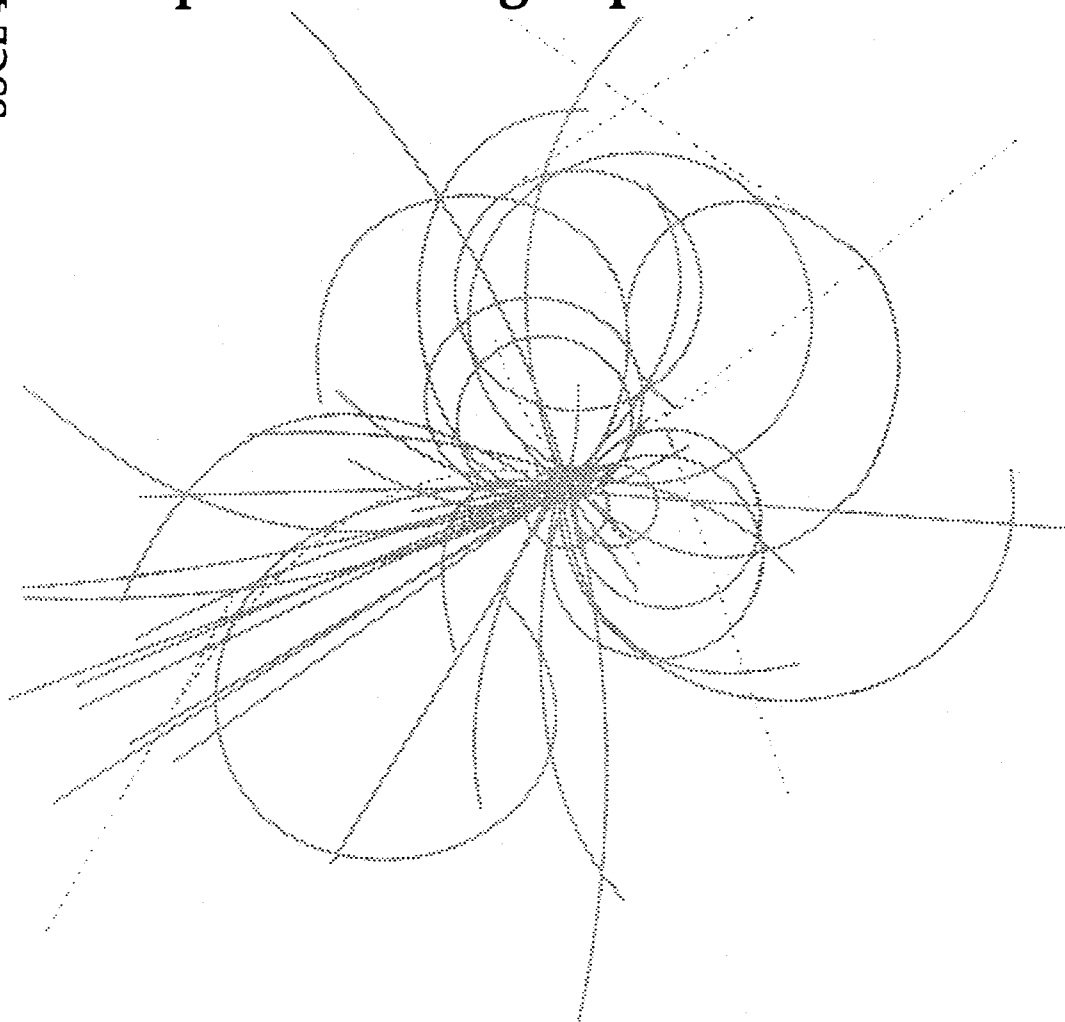# Superconducting Super Collider Laboratory

Using the Top Quark for Testing Standard Model Polarization and CP Predictions

G.L. Kane, G. A. Ladinsky, and C.-P. Yuan

June 1991

Using the Top Quark for
Testing Standard Model Polarization and CP Predictions

G.L. KANE

Randall Physics Laboratory, University of Michigan, Ann Arbor, MI 48109

and

SSC Laboratory, Dallas, TX 75237[*]

G.A. LADINSKY

Department of Physics, 104 Davey Laboratory
The Pennsylvania State University, University Park, PA 16802

C.-P. YUAN[†]

Institute for Particle Physics, University of California, Santa Cruz, CA 95064

and

Department of Physics and Astronomy,
The Johns Hopkins University, Baltimore, MD 21218

Abstract

Once top quarks are found, because they are heavy they will allow many new tests of the Standard Model and new probes of physics at the 100 GeV scale. In this paper we show how to test the Standard Model QCD predictions for the transverse polarization of a top quark produced at the Tevatron, SSC, LHC and NLC. We also examine the most general form of the $W - t - b$ vertex, and show how to detect effects of non–SM operators. Ways of detecting non–SM CP violation effects in either the production or the decay of the top and anti–top quarks are examined.

Submitted to *Physical Review D*

---

1. Introduction

Recently, the top quark has been found to be heavier than 45 GeV from SLAC and LEP experiments[1] and 89 GeV from CDF data.[2] The first limit is model independent while the second limit is for the Standard Model (SM) top quark. Since the top quark is heavy, of the same order of magnitude as the W–boson mass, any physical observable which is related to the top quark may be sensitive to new physics. (We use W–boson to denote either $W^{\pm}$ or Z^0 unless specified otherwise.)

Studying top quarks may be particularly interesting for several practical reasons in addition to the general one that it probes physics at a much higher mass scale than other fermions. Because it is heavy, energy conservation may allow non–SM decays that signal new physics. For our purposes in this paper, the most important consequence of a heavy top quark is that to a good approximation it decays as a free quark, since its lifetime is $\tau \sim 1.2(M_W/m_t)^3$ fermis, and it does not have time to bind with light quarks before it decays. Thus we can use the polarization properties of the top quark as additional observables for testing the Standard Model and to probe for new physics.

Further, because the top quark will have the weak two–body decay $t \to bW^+$, it will analyze its own polarization. Top quarks will have longitudinal polarization if weak effects are present in their production, but they also can have polarization transverse to the production plane. It was first noticed long ago[3] that at tree level the produced $q\bar{q}$ in e^+e^- or hadron collisions can not be transversely polarized because transverse polarization can arise only from the interference of complex helicity flip and non–flip amplitudes, while at tree level the amplitudes are relatively real. Including one–loop gluon contributions, the degree of transverse polarization of the quark q produced from $e^-e^+ \to q\bar{q}$ is

$$P_{\perp} = K\alpha_s \frac{m_q \beta}{\sqrt{S}} f(\theta), \qquad (1.1)$$

where α_s arises from the loop, the quark mass m_q occurs because one amplitude must be helicity flip, $\beta = \sqrt{1 - 4m_q^2/S}$, K is a number of order unity, and $f(\theta)$ is a function of the production angle. $\sqrt{S}$ is the center of mass energy of the $q\bar{q}$ system. K and $f(\theta)$ are different for e^-e^+ and hadron collisions, and are given below.

For light quarks $P_{\perp}$ is effectively zero numerically. Unfortunately, it is not easy to test this prediction because it is not known how to measure light quark polarizations. In particular, once quarks bind into hadrons there is no understanding of

how spin effects behave. For heavy top quarks measuring $P_\perp$ may be possible, as we describe below, and the top quark mass m_t is large enough so that a non–zero $P_\perp$ may be detectable, though we will see that $P_\perp$ is not very large even for a SM top quark.

It should be emphasized that transverse polarization studies provide an important QCD test since the leading behavior of $P_\perp$ is governed by one loop QCD contributions (rather than having the QCD loop diagrams enter as a small numerical correction to a tree level effect), and $P_\perp$ depends on the phase of the loop contribution.

With the large production rate expected for top quarks at the SSC and LHC, it will be possible to make a very detailed study of the interactions of the top quark, including polarization effects. If new interactions occur, they may manifest themselves in an enhancement of the polarization effects in the production of the top quark.

The decay of the top quark could be sensitive to new physics as well as the production of the top quark. In the top quark decay it is important to examine the different types of operators the $W - t - b$ vertex might involve. For instance, one should examine the form factors which result from an effective lagrangian obtained by higher order QCD effects.[4] One may also examine the form factors to test the plausibility of having the *nonuniversal* gauge couplings[5] of $W - t - b$ due to some dynamical symmetry breaking scenario.

In this paper, we discuss how to detect the transverse polarization of the top quark. Assuming the $W - t - b$ coupling is standard, we show how to test QCD at the loop level by examining the polarization of the top quark which is produced mainly from the process $gg \to t\bar{t}$ at the SSC or LHC. We also study the general $W - t - b$ form factors while assuming the production mechanism agrees with the SM prediction. In the decays $t \to W^+b$ (or $\bar{t} \to W^-\bar{b}$) one can study the $W - t - b$ form factors through the angular distribution and the percentage of the longitudinal W–bosons produced in the rest frame of the top (or anti–top) quarks.

In addition, methods for detecting possible CP violations in either the production or decay process are given. Although Standard Model CP violation effects (from the Cabibbo–Kobayashi–Maskawa mixing angles) will be small for both the production and decay of the top quark, it is important to test for CP violation because it could arise from new physics; no CP studies have been done at the 100 GeV scale.

This paper is organized as follows. In Section 2, we discuss how to test QCD at the loop level. In Section 3, methods to study the $W - t - b$ form factors are given. Section 4 discusses possible CP violation in the production process. A similar

3

discussion for the decay process is given in Section 5. $e^- e^+ \to t\bar{t}$ is discussed in Section 6. Section 7 contains some conclusions.

2. Testing QCD at Hadron Colliders

For a 140 GeV SM top quark, the production rate for a $t\bar{t}$ pair from the QCD processes

$$gg \to t\bar{t} \quad \text{and} \quad q\bar{q} \to t\bar{t} \qquad (2.1)$$

is about 10^8 events per SSC year (10^4pb^{-1} integrated luminosity) corresponding to a cross section of 1.1nb. At the LHC it is about 5 to 6 times smaller. It is possible to test QCD at the loop level with such a generous sample of top quark events. We follow the ideas in Ref. 3 and study the transverse polarization of the top quark to test QCD beyond tree level. In this paper when we write *polarization* we mean transverse polarization unless specified otherwise.

Since the QCD interaction is C (Charge Conjugation) and P (Parity) invariant, the produced top quark from the processes in (2.1) can only be transversely polarized. At tree level, the produced top quark is not polarized because the tree amplitude for production is real. At the loop level, however, it is possible to generate an imaginary part in the scattering amplitude so that the top quark is transversely polarized. The degree of polarization of the top quark from the gg fusion process can be obtained from the formula given in Ref 6.

To simplify the argument, we use the parton level results and ignore detector effects. The correlations between the W^+ and W^- bosons from t and $\bar{t}$ decay will be emphasized because they are sensitive to new physics. Since none of the most popular general purpose Monte Carlo programs have such correlation effects implemented, our parton level analysis should be more reliable for studying the weak decay[7] of a heavy top quark if both the initial and final state gluon radiation effects are ignored. Although the effects from gluon radiation might be large, the general ideas presented in this paper will remain valid when a higher order analytic calculation is available. In our work, we use the tree level results with the general form factors included when we discuss the correlations between the W^+ and W^- gauge bosons. When we discuss the transverse polarization of the top quark, the one loop results from the QCD corrections will be used.

We assume a narrow width approximation for the top quark decay. The method[8-10] is to calculate the helicity amplitudes, and then square the amplitudes numerically including some kinematics cuts to be introduced later in this section. We follow closely the notation in Ref 8. The scattering plane is chosen as the $X - Z$ plane; the top quark is therefore polarized along the $\pm Y$ direction. A

4

study[11,12] of the next to leading order QCD corrections to the processes in (2.1) suggests that the kinematics of the top quark can be reasonably reproduced from the Born process results multiplied by a suitable K—factor. Even though this K–factor varies somewhat with the transverse momentum (P_T) and rapidity (y) of the top quark,[12,13] we ignore such a dependence in our study and use the tree amplitudes listed in Appendix A. In this section we assume the weak decays of the top and anti–top quarks are standard. The helicity amplitudes for the decay process $t \to bW^+$ can be obtained from the results listed in Appendix B.

The degree of transverse polarization of the top quark is derived from the imaginary part of the production amplitudes. Since this contribution to the cross section enters at next to leading order in α_s, its effect on the kinematics is small provided the cross section is scaled by a suitable K–factor. When using it to determine polarization effects, one is comparing this contribution to the zero polarization given by the Born amplitudes. We therefore use the Born result to simulate the kinematics of the top quark and implement the polarization matrix of the top quark to generate the correct kinematics for a polarized top quark decay. We calculate the weighted amplitude squared decomposed over an helicity basis through the sum

$$
\begin{aligned}
|M(gg \to t\bar{t} \to bW^+\bar{b}W^-)|^2 &= \sum_{\lambda,\bar{\lambda}} |M(gg \to t_\lambda \bar{t}_{\bar{\lambda}})|^2 \\
&\times \sum_{\lambda',\lambda} M^\dagger(t_{\lambda'} \to bW^+) \rho_{\lambda'\lambda} M(t_\lambda \to bW^+) \\
&\times \sum_{\bar{\lambda},\bar{\lambda}'} M(\bar{t}_{\bar{\lambda}} \to \bar{b}W^-) \bar{\rho}_{\bar{\lambda}\bar{\lambda}'} M^\dagger(\bar{t}_{\bar{\lambda}'} \to \bar{b}W^-)
\end{aligned}
\tag{2.2}
$$

where the top quark polarization matrix, $\rho_{\lambda'\lambda}$, is parametrized as[9]

$$
\rho_{\lambda'\lambda} = \frac{1}{2} \begin{pmatrix} 1 + P_\| & P_\perp e^{i\alpha} \\ P_\perp e^{-i\alpha} & 1 - P_\| \end{pmatrix},
\tag{2.3}
$$

and the anti–quark polarization matrix is written as

$$
\bar{\rho}_{\bar{\lambda}\bar{\lambda}'} = \frac{1}{2} \begin{pmatrix} 1 + \overline{P}_\| & \overline{P}_\perp e^{-i\bar{\alpha}} \\ \overline{P}_\perp e^{i\bar{\alpha}} & 1 - \overline{P}_\| \end{pmatrix}.
\tag{2.4}
$$

We have checked that the Eq. (7.7b) in Ref. 9 is also true for a massive fermion. In QCD, $P_\| = \overline{P}_\| = 0$, $P_\perp = \overline{P}_\perp$, and $\alpha = -\bar{\alpha} = \pi/2$ if the top quark is polarized along the $+Y$ direction in the center of mass frame of $t\bar{t}$. For completeness, we

summarize our notation about the polarization matrix in Appendix C. The degree of polarization given in Ref. 6 is $P_\perp \sin\alpha$ in our notation. Strictly speaking, Eq. (2.2) is invalid when the correlation effects between the W^+ and W^- bosons are important. In principle, if we calculate the helicity amplitudes of the gluon fusion process in (2.1) up to one loop order, then we can use

$$
\begin{aligned}
|M(gg \to t\bar{t} \to bW^+\bar{b}W^-)|^2 = \sum_{\lambda,\bar\lambda} \sum_{\lambda',\bar\lambda'} &M^\dagger(gg \to t_{\lambda'}\bar{t}_{\bar\lambda'})M(gg \to t_\lambda\bar{t}_{\bar\lambda}) \\
&\times M^\dagger(t_{\lambda'} \to bW^+)M(t_\lambda \to bW^+) \\
&\times M^\dagger(\bar{t}_{\bar\lambda'} \to \bar{b}W^-)M(\bar{t}_{\bar\lambda} \to \bar{b}W^-)
\end{aligned}
\tag{2.5}
$$

to obtain the correct correlation effects between W^+ and W^- due to the polarization of the top and anti-top quarks. Instead of doing this, we use the result given in Ref. 6 to obtain the degree of transverse polarization of the top quark produced via the gluon fusion process in (2.1), and discuss methods to test that prediction. Eq. (2.2) is sufficient as long as we do not use it to study the correlation effects. In Section 3, we use Eq. (2.5) to study the correlation effects between W^+ and W^- at the tree level with the most general $W - t - b$ form factors included.

In Fig. 1 we display the polarization for a 140 GeV top quark produced from the gluon fusion process. Specifically, we have plotted the transverse polarization, $P_\perp \sin\alpha$, of the top quark as a function of its polar angle (θ_t) and for various top quark energies (E_t) in the $t\bar{t}$ center of mass frame. We note that the top quark is polarized along the $+Y$ direction when θ_t is less than $\pi/2$ and along the $-Y$ direction otherwise. Selecting which direction is the direction of positive Z is arbitrary. Taking advantage of the identical particle symmetry of the initial gg state, we may use our definition that the scattering plane be the $X - Z$ plane and set $\phi_t = 0$. In other words, we always set our coordinates such that the top quark is within the $+X$ half of the $X - Z$ plane. The θ_t distribution for a 140 GeV top quark produced via the gluon fusion process at the SSC is shown in Fig. 2.

Unless specified otherwise, in all the figures shown in this paper we impose kinematic cuts on the transverse momentum P_T and rapidity y of all the visible final state partons. Also, we demand a minimum $\Delta R_{ij} = \sqrt{(\Delta y_{ij})^2 + (\Delta \phi_{ij})^2}$ separation between any two of the visible final state partons i and j. ϕ is the azimuthal angle measured in the lab frame. The cuts are

$$
P_T \geq 30\,\text{GeV}, \qquad |y| \leq 2.5, \qquad \text{and} \qquad \Delta R_{ij} \geq 0.5
\tag{2.6}
$$

as taken in the lab frame. We use the leading order fit, Fit SL in table III3, of the parton distribution functions given by Morfin and Tung.[14]

Our purpose is to measure the transverse polarization of the top quarks, $P_\perp$. In Eq. (B.2) of Appendix B we present the decay amplitudes for top quarks and we have explicitly expressed the dependence of this decay according to the helicity of the produced W–boson. The lowest order contributions to these decay amplitudes for a SM top quark are given by the terms that depend on f_1^L. The other relevant form factor, f_2^R, contains only higher order corrections, so its contribution is expected to be suppressed by $O(\alpha_s)$ compared to the f_1^L. Examining these amplitudes further, we find an enhancement of the lowest order contributions by a factor of (m_t/M_W) exists for the case where the top quark decays into longitudinally polarized W–bosons as compared to the production of W–bosons with transverse polarizations. For these reasons we decide to focus our attention on the study of longitudinal W–bosons.

As shown in Appendix B, the angular distribution of the longitudinal W^+ boson produced from a SM top quark decay in the rest frame of t is

$$1 + P_\perp \sin\theta_W \sin\phi_W \tag{2.7}$$

if the top quark is polarized along the $+Y$ direction and where θ_W (ϕ_W) is the polar (azimuthal) angle of the W^+ boson measured in the rest frame of the top quark. In this frame the $+Z$ direction is defined to be the moving direction of the top quark in the center of mass frame of the $t\bar{t}$ system. Thus, the longitudinal W–boson from a transversely polarized top quark decay tends to move along the direction of the top quark polarization, as indicated in (2.7).

Since the degree of transverse polarization ($P_\perp$) in the QCD reaction is small, of the order of a few percent, it is not easy to measure $P_\perp$. One possibility is to weight each event by $\sin\phi_W$. Because the kinematic cuts in (2.6) are unlikely to bias the azimuthal distribution, the weighted integration over $\sin\phi_W$ will make the first term in Eq. (2.7) vanish if this integration is complete from 0 to 2π, while the second term gives a distribution like

$$\frac{1}{2} P_\perp \sin\theta_W. \tag{2.8}$$

From this distribution we can measure $P_\perp$ if it is large enough. It should be emphasized that $P_\perp$ is a good observable to test for QCD loop effects since it is zero at the tree level in the SM and calculable, though small, from higher order perturbative QCD. If a large value of $P_\perp$ were observed, it would directly imply the existence of large non-SM effects without the need for distinguishing the SM part.

7

To illustrate the use of this method, we assume that $P_\perp$ is as large as one and that the t is polarized up (along the $+Y$ direction) when $\theta_t < \pi/2$, and down (along the $-Y$ direction) when $\theta_t > \pi/2$. The weak decays of t and $\bar{t}$ are taken to be standard. From Eq. (B.2) we can obtain the ratio of the fraction of longitudinal versus transverse W^+ bosons

$$\frac{\overline{|M(\lambda_W = 0)|}^2}{\overline{|M(\lambda_W = -)|}^2} = \frac{m_t^2}{2M_W^2} \frac{1 + P_\perp \sin\theta_W \sin\phi_W}{1 - P_\perp \sin\theta_W \sin\phi_W} \qquad (2.9)$$

for a SM top quark polarized upward. (At tree level, the only nonvanishing form factor is $f_1^L = 1$.) To optimize the efficiency of this method, we first select the samples with t polarized up by imposing

$$\theta_t < \pi/2 \qquad (2.10)$$

in the center of mass frame of $t\bar{t}$. This is not a cut, but merely a selection of the orientation for our coordinate axes, since the identical particle symmetry of the gg initial state always allows us to put the top quark in the first quadrant. We then enhance the samples with longitudinal W's from t decay by imposing

$$|\cos\theta_{e^+}^*| < 0.6, \qquad (2.11)$$

where $\theta_{e^+}^*$ is the polar angle of the e^+ defined in the rest frame of the W^+ boson. The $+Z$ axis of this frame is chosen to be opposite to the b quark direction in the rest frame of the top quark for the decay $t \to bW^+ \to be^+\nu_e$. The distribution of $\theta_{e^+}^*$ for a polarized W^+ boson can be obtained from Eq. (B.3). In Fig. 3(a), we show the distribution of $\cos\theta_{e^+}^*$ for an unpolarized 140 GeV SM top quark before the cuts (2.6). As shown in Fig. 3(b), after the cuts (2.6) the fraction of longitudinal W^+ bosons is enhanced, i.e., the W decay is more like $\sin^2\theta_{e^+}^*$. This can be understood from Eqs. (B.2) and (B.3) because a SM top quark can only decay into either a longitudinal or a left–handed W^+ boson in the limit of taking the bottom quark mass m_b to be zero. A left–handed W^+ boson tends to decay to an e^+ moving toward the b direction in the t rest frame so that the kinematic cuts in Eq. (2.6) degrade the sampling of such events. Note, however, that the cuts in Eq. (2.6) distort the distribution somewhat, so the plot in Fig. 3(b) is not quite $\sin^2\theta_W$.

After imposing Eq. (2.10) and the cuts in Eqs. (2.6) and (2.11), we get the weighted θ_W distribution shown in Fig. 4 for a completely transversely polarized 140 GeV SM top quark produced from the gluon fusion process at the SSC. The number of $t\bar{t}$ pairs in the plot is 8×10^6. The area under the curve in Fig. 4 is

proportional to the degree of polarization $P_\perp$. (A similar analysis can be applied to measure $\overline{P}_\perp$ of $\bar{t}$.) At the SSC, the number of events that survive the cuts in Eq. (2.6) is 9.4% for a 140 GeV top quark, and 80% for the cut in Eq. (2.11) while imposing Eq. (2.10). Therefore, after the cuts in Eq. (2.6), there are about 10^7 $t\bar{t}$ pairs produced at the SSC via the gluon fusion process.

So far, we have only considered the $P_\perp$ contribution from the gluon fusion process. The contribution from quark–antiquark annihilation should also be included. The Born helicity amplitudes for this process are given in Appendix A. From Fig. 1 we find that the degree of polarization $P_\perp$ becomes smaller for much larger top quark energies. In addition, the cross section decreases for larger invariant masses of the $t\bar{t}$ pair ($M_{t\bar{t}}$), and the gluon fusion process dominates the production of $t\bar{t}$ at smaller $M_{t\bar{t}}$ for either the SSC or the LHC. Hence, neglecting the $q\bar{q}$ contribution to the polarization should be a reasonable approximation for the SSC and LHC. However, the dominant production mechanism for a heavy top quark (≥ 100 GeV) at the Tevatron is the $q\bar{q}$ process. In Fig. 5 we show the Born cross sections for both the gluon–gluon fusion and quark–antiquark annihilation processes in (2.1) at the SSC, LHC and Tevatron. (No branching ratios are included.) The $\overline{MS}$ scheme to first order in α_s is used, and the scale to evaluate the parton distribution functions is chosen to be the transverse mass of the top quark, $\sqrt{m_t^2 + P_T^2}$. No kinematic cuts are imposed. Note that the next to leading order QCD corrections will increase the cross section of the gg fusion process more than that of the $q\bar{q}$ fusion process for the production of heavy top quarks at the SSC or LHC.[11,12]

Since the one loop QCD result for the transverse polarization of the top quark produced from the gluon fusion process in (2.1) is only a few percent in magnitude, as shown in Fig. 1, it may be difficult to observe even at the SSC or the LHC. The top quark may be discovered at the FNAL. If so, several thousand top quarks will be produced there. That is not enough to allow a real measurement of the top quark polarization, but it will still be interesting and important at FNAL to study polarization effects, and to check that large polarizations do not occur; if $P_\perp$ should be large, it would signal new physics beyond the SM.

To summarize, experimentalists should take a sample of top quark events, impose Eq. (2.10) and the cuts in Eqs. (2.6) and (2.11), and weight the events by $\sin \phi_W$. They should then plot the number of events vs. θ_W. A $\sin \theta_W$ distribution should result whose peak height is proportional to $P_\perp$, where $P_\perp$ is given in Fig. 1 for the constituent processes (and has to be convoluted with the gluon structure function to get the result for the appropriate hadron collider).

3. Testing the Coupling of W^+bt

In the previous section we showed how to test QCD at the loop level by examining the transverse polarization of the top quark under the assumption that the decay of the top quark is described by the SM. However, the top quark is heavy, so it is possible that new physics may appear in a physical observable associated with the top quark. For example, recently[5] it has been suggested that the top quark may have nonuniversal gauge couplings due to some dynamical symmetry breaking scenario. In this section we study the decay process

$$t \to W^+b \tag{3.1}$$

using the most general form factors to describe the interaction assuming the W-boson and bottom quark (b) are on-shell.

The QCD[4] and electroweak[15] corrections to the decay process in (3.1) in the SM have been done recently. In this section, we study the most general operators for this coupling, which is described by the interaction lagrangian

$$L = \frac{g}{\sqrt{2}} \left[W_\mu^- \bar{b}\gamma^\mu(f_1^L P_- + f_1^R P_+)t - \frac{1}{M_W}\partial_\nu W_\mu^- \bar{b}\sigma^{\mu\nu}(f_2^L P_- + f_2^R P_+)t \right]$$
$$+ \frac{g}{\sqrt{2}} \left[W_\mu^+ \bar{t}\gamma^\mu(f_1^{L*} P_- + f_1^{R*} P_+)b - \frac{1}{M_W}\partial_\nu W_\mu^+ \bar{t}\sigma^{\mu\nu}(f_2^{R*} P_- + f_2^{L*} P_+)b \right],$$
$$\tag{3.2}$$

where $P_\pm = \frac{1}{2}(1\pm\gamma_5)$, $i\sigma^{\mu\nu} = -\frac{1}{2}[\gamma^\mu, \gamma^\nu]$ and the superscript $*$ denotes the complex conjugate. In general, the form factors $f_1^{L,R}$ and $f_2^{L,R}$ can be complex. If the W-boson can be off-shell then there are additional form factors such as

$$\partial^\mu W_\mu^- \bar{b}(f_3^L P_- + f_3^R P_+)t + \text{h.c.} \tag{3.3}$$

which vanish for an on-shell W-boson or when the off-shell W-boson couples to massless on-shell fermions. We only consider on-shell W-bosons, assuming that $m_t > M_W + m_b$. At tree level in the SM the form factors are $f_1^L = 1$ and $f_1^R = f_2^L = f_2^R = 0$. We want to study the effects of these form factors on the experimental observables related to the top quark. For example, there will be effects on the fraction of longitudinal W's produced in top quark decays. To simplify our discussion in this section, we use the Born processes in (2.1) to generate the top quark kinematics and ignore the small transverse polarization of the top quark due to the QCD radiative corrections beyond the tree level. Namely, we use Eq. (2.5) for this study. The helicity amplitudes for the production processes in (2.1) and the subsequent decays in (3.1) are given in Appendices A and B,

10

respectively. In addition, in the rest frame of the top quark, the probability of producing a right–handed, left–handed, or longitudinal W–boson is also given in Appendix B. Note that if f_1^R were as big as f_1^L, then it would contribute the same amount of longitudinal W's as f_1^L. Therefore, we need to examine the correlation between the W^+ from the top quark decay and the W^- from the anti–top quark decay to untangle these four form factors. In reality, kinematic cuts like Eq. (2.6) will be imposed in analyzing a data sample. These cuts might bias the polarization of the W–boson (cf. Fig. 3(a,b)), so we perform this analysis using a Monte Carlo method instead of an analytical calculation.[16]

The fraction (f_L) of longitudinally polarized W–bosons produced in the rest frame of the decaying top quarks strongly depends on the form factors $f_1^{L,R}$ and $f_2^{L,R}$, as shown in Appendix B, making f_L a useful observable for measuring these form factors. The definition of f_L is simply the ratio of the number of longitudinally polarized W–bosons produced with respect to the total number of W–bosons produced in top quark decays:

$$f_L = \frac{\Gamma(\lambda_W = 0)}{\Gamma(\lambda_W = 0) + \Gamma(\lambda_W = -) + \Gamma(\lambda_W = +)} \tag{3.4}$$

where we use $\Gamma(\lambda_W)$ to refer to the decay rate for a top quark to decay into a W–boson with polarization λ_W. Eq. (2.9), which gave the ratio of the number of longitudinally polarized W–bosons to transversely polarized W–bosons at tree level in the SM, was a specific case of $f_L(1 - f_L)^{-1}$.

In Section 2 we mentioned that the form factors for a SM top quark decay were such that the leading behavior was given by f_1^L. This indicated an enhancement of the production of W–bosons with longitudinal polarizations in the SM top quark decays. This behavior is representative of the models usually considered in particle physics, where the longitudinal mode of the W–bosons, as generated through spontaneous symmetry breaking, have a coupling which increases with the fermion mass. Remaining open to the possibility of new physics, however, it is conceivable that the form factors could be similar in magnitude or even that $|f_1^L| < |f_2^R|$ and/or $|f_1^R| < |f_2^L|$. If this were the case, then from inspection of Eq. (B.2), we should expect a significant proportion of transversely polarized W–bosons produced in top decays, perhaps exceeding the number of longitudinally polarized W–bosons produced. It would then be efficient to examine the fraction of transversely polarized W's and to use their distributions in investigating the degree of polarization for the top quark. In such studies, we would need to replace cuts like Eq. (2.11) with complementary cuts designed to enhance the number of transverse W's. The general procedure for studying the top quark would still be the same, so we assume the form factors do not vary too radically from the SM physics and focus on f_L.

11

To find f_L, we follow the method used in our previous work[17] and calculate the polar angle $\theta_{e^+}^*$ distribution of the e^+ in the rest frame of the W^+ boson whose Z–axis is defined to be the moving direction of the W^+ boson in the rest frame of the top quark:

$$
\begin{aligned}
\cos \theta_{e^+}^* &= \frac{p_e \cdot p_b - E_e E_b}{|\vec{p}_e||\vec{p}_b|} \\
&\simeq \frac{p_e \cdot p_b}{E_e E_b} - 1 = \frac{2M_{eb}^2}{m_t^2 - M_W^2} - 1.
\end{aligned}
\tag{3.5}
$$

The energies E_e and E_b are evaluated in the rest frame of the W^+ boson from the top quark decay and are given by

$$
\begin{aligned}
E_e &= \frac{M_W^2 + m_e^2 - m_\nu^2}{2M_W}, & |\vec{p}_e| &= \sqrt{E_e^2 - m_e^2}, \\
E_b &= \frac{m_t^2 - M_W^2 - m_b^2}{2M_W}, & |\vec{p}_b| &= \sqrt{E_b^2 - m_b^2}.
\end{aligned}
\tag{3.6}
$$

where M_{eb} is the invariant mass of eb. m_e (m_ν) denotes the mass of e^+ (ν_e) for the sake of bookkeeping. The first line in Eq. (3.5) is exact when using Eq. (3.6), while the second line of Eq. (3.5) holds in the limit of $m_b = 0$. Taking the $\cos \theta_{e^+}^*$ distribution and fitting it according to the amplitudes given by Eq. (B.3) yields f_L.

Another useful observable is the angular correlation between the W^+ and the W^-. We must take care, however, for if we were to use a formula analogous to Eq. (2.2) for computing the amplitude, we would lose the information which would be transferred between the production of the top and anti–top quarks and their subsequent decays. Instead, we use the formula given in Eq. (2.5) for $gg \to t\bar{t} \to bW^+\bar{b}W^-$ and maintain the correlations between the top and anti–top quark decays. To simplify our discussion, let us consider the specific helicity state with $h_{g1} = h_{g2} = -$ and $\lambda_{W^+} = \lambda_{W^-} = 0$ for a nonvanishing f_1^L and f_2^R in the limit of $m_b = 0$. (This is the case for considering SM corrections to the decay process in (3.1).) Using the helicity amplitudes for $t\bar{t}$ production, $(h_{g1}, h_{g2}, h_t, h_{\bar{t}})$ as in Eq. (A.2), the amplitude for this specific helicity state is (ignoring some overall factors given in the appendices)

$$
\begin{aligned}
M(g_{h_{g1}} g_{h_{g2}} &\to t\bar{t} \to bW^+_{\lambda_{W^+}} \bar{b}W^-_{\lambda_{W^-}}) \\
&\propto (----)(-0-)\overline{(-0+)} + (---+)(-0-)\overline{(+0+)} \\
&\quad + (--+-)(+0-)\overline{(-0+)} + (--++)(+0-)\overline{(+0+)}.
\end{aligned}
\tag{3.7}
$$

In this formula $(-0-)$ and $(+0-)$ are the helicity amplitudes for t decay,

12

$(h_t, \lambda_{W^+}, h_b)$, which are given in Eq. (B.1) while $\overline{(-0+)}$ and $\overline{(+0+)}$ are the helicity amplitudes for $\bar{t}$ decay, $\overline{(h_{\bar{t}}, \lambda_{W^-}, h_{\bar{b}})}$, which can be obtained from Eq. (B.1) after the proper substitutions discussed below Eq. (B.2).

Apart from the dependence on the energy (E_t) and polar angle (θ_t) of the top quark in the center of mass frame of $t\bar{t}$, one of the interference terms from the square of Eq. (3.7) contains the factor

$$- \left| \frac{m_t}{M_W} f_1^L + f_2^R \right|^4 \sin \theta_{W^+} \sin \theta_{W^-} \cos(\phi_{W^+} + \phi_{W^-}). \tag{3.8}$$

The definition of θ_W and ϕ_W are similar to the definition of $\theta^*_{e^+}$ given in the previous section, i.e., θ_{W^+} (ϕ_{W^+}) is the polar (azimuthal) angle of the W^+ boson in the rest frame of the top quark. The $+Z$ axis of this frame is opposite to the $\bar{t}$ direction in the center of mass frame of the $t\bar{t}$ system. All of these angles are defined using a right–handed coordinate system. If we express θ_{W^-} and ϕ_{W^-} in a reference frame which is parallel to the rest frame of the top quark, then in Eq. (3.8) θ_{W^-} should be replaced by $\pi - \theta_{W^-}$ and ϕ_{W^-} by $\pi - \phi_{W^-}$ because the Y-axis is fixed to be perpendicular to the scattering plane and the Z axis of the anti–top quark rest frame is opposite to the Z axis of the top quark rest frame in the center of mass frame of $t\bar{t}$.

In Eq. (3.8), the factor $\cos(\phi_{W^+} + \phi_{W^-})$ produces a correlation between W^+ and W^- in their azimuthal distributions. We see that this effect grows as the top quark becomes heavier, as shown in Eq. (3.8). In Fig. 6(a), we show the difference between the results obtained from the correlated amplitude in Eq. (2.5) and the uncorrelated amplitude in Eq. (2.2) for unpolarized 140 GeV SM $t\bar{t}$ pairs produced from the gluon fusion process in the distribution of

$$\Delta\phi_W^{lab} = \phi_{W^+}^{lab} - \phi_{W^-}^{lab}. \tag{3.9}$$

The superscript lab indicates that ϕ is defined in the lab frame. The range of $\Delta\phi_W^{lab}$ is chosen to be from 0 to 2π because the different charges of W^+ and W^- make the two gauge bosons distinguishable. The kinematic cuts in Eq. (2.6) are not imposed, but we do enrich the events sampled with longitudinal W's by imposing Eq. (2.10) along with the cuts Eq. (2.11),

$$|\cos \theta^*_{e^-}| < 0.6, \tag{3.10}$$

$$|\cos \theta_{W^+}| < 0.4, \quad \text{and} \quad |\cos \theta_{W^-}| < 0.4 \tag{3.11}$$

making the correlation effects of interest more pronounced. For a 140 GeV top quark produced at the SSC via the gluon fusion process, the number of events

which survive all the cuts in Eqs. (2.10), (2.11), (3.10), (3.11), is about 7.4% if the cuts in Eq. (2.6) were not imposed, and 14% if the cuts in Eq. (2.6) were imposed. With this last result about 10^6 $t\bar{t}$ pairs survive these kinematic constraints at the SSC. The difference plotted in Fig. 6(a) is small[18] though the difference grows with m_t. So, the results we draw from Eq. (2.2) should be reasonable for a 140 GeV top quark. For comparison, we also show the $\Delta\phi_W^{lab}$ distribution obtained from Eq. (2.5) in Fig. 6(b). We found that the difference between the results obtained with the correlated and uncorrelated computations reaches the maximum, about 5%, when $\Delta\phi_W^{lab} = \pi$. Qualitatively, we find the correlated amplitude of Eq. (2.5) will produce fewer back–to–back gauge bosons in the transverse plane perpendicular to the beam axis compared to the uncorrelated amplitude of Eq. (2.2).

Using Eqs. (B.1) and (B.2) one can find distributions to untangle all the different form factors associated with the $W - t - b$ interaction. If the top quark is polarized, further use can be made of equation (B.2) to untangle the form factors by measuring f_L as a function of θ_W and ϕ_W. The next paragraph describes one method to extract these form factors.

As described in the previous section, we assume that $P_\perp$ is as large as one and that t is polarized up (along the $+Y$ direction) when $\theta_t < \pi/2$, and down (along the $-Y$ direction) when $\theta_t > \pi/2$. The weak decays of t and $\bar{t}$ are taken to be standard. From Eq. (B.2) we found that the longitudinal W^+ boson from t decay tends to move along the top quark polarization direction. This is obvious for $\alpha = \pi/2$ in Eq. (B.2). After the appropriate substitutions as described in Appendix B, we obtain the angular distribution of the longitudinal W^- bosons from polarized $\bar{t}$ decays,

$$\overline{|M(\lambda_{W^-} = 0)|}^2 = \frac{1}{2}\left|\frac{m_t}{M_W}f_1^R + f_2^L\right|^2 \left[1 + \overline{P}_{||}\cos\theta_{W^-} + \overline{P}_\perp\sin\theta_{W^-}\cos(\bar{\alpha} - \phi_{W^-})\right]$$
$$+ \frac{1}{2}\left|\frac{m_t}{M_W}f_1^L + f_2^R\right|^2 \left[1 - \overline{P}_{||}\cos\theta_{W^-} - \overline{P}_\perp\sin\theta_{W^-}\cos(\bar{\alpha} - \phi_{W^-})\right].$$

(3.12)

Let us assume that the $t\bar{t}$ production mechanism is CP invariant so that the degree of transverse polarization of $\bar{t}$ is the same as that of t, $\overline{P}_\perp = P_\perp$, and the polarization direction of $\bar{t}$ is opposite to that of t. For instance, when t is polarized up (along the $+Y$ direction, $\alpha = \pi/2$), $\bar{t}$ is polarized down (along the $-Y$ direction, $\bar{\alpha} = -\pi/2$,). From Eq. (3.12) we found that the W^- boson from the $\bar{t}$ decay tends to move opposite to the polarization direction of $\bar{t}$. (We again assume $\overline{P}_{||} = P_{||} = 0$ for simplicity.) Hence, if both the t and $\bar{t}$ are transversely polarized, the produced W^+ and W^- will tend to move along the same direction, becoming less back–to–back in the transverse plane perpendicular to the beam axis. (This therefore

14

provides a method to test for CP violation in the $t\bar{t}$ production, to which we will return in the next section.) To *estimate* the effect of such correlations between W^+ and W^-, we use Eqs. (2.2), (2.3) and (2.4) to calculate the $\Delta\phi_W^{lab}$ distribution for a completely transversely polarized t and $\bar{t}$. The difference in the $\Delta\phi_W^{lab}$ distributions between this completely polarized and the previously unpolarized case is shown in Fig. 7 for a 140 GeV SM $t\bar{t}$ pair produced from the gluon fusion process at the SSC. We conclude that for a polarized $t\bar{t}$ pair the W^+ and W^- are less back–to–back in the transverse plane perpendicular to the beam axis than in the case where the $t\bar{t}$ pair is unpolarized. To obtain Fig. 7, we imposed cuts similar to those of Fig. 6.

We shall not do any further numerical analysis but point out that by measuring the fraction (f_L) of the longitudinal W^+ (W^-) from t $(\bar{t})$ decay and the angular correlations between W^+ and W^- one can extract all the effects due to these form factors provided they are not very small. Instead of giving the analytic expression of these correlations we have presented all the relevant helicity amplitudes in Appendices A and B so that they can be easily implemented in an event generator with the flexibility of imposing any sort of kinematic cuts. In practice, this will bias the polarization of the W–boson somewhat. In section 5, we describe another method for measuring these form factors.

Finally, we note that when measuring these form factors one has to consider the possible interference effects[19] from any two of them. For instance, as indicated in Eq. (3.8), the interference of f_1^L and f_2^R contributes to the ϕ correlations of W^+ and W^-.

We have demonstrated several means which are available for studying general top quark decays. This gains in importance as we realize this to be a hunting ground for new physics. With the high top quark mass, the potential for strong polarization effects is present. Using Monte Carlo methods, we have seen that in the center of mass frame of a polarized $t\bar{t}$ pair that the resultant W^+ and W^- are produced less back–to–back than in the unpolarized case, providing us with an important signal provided the polarization of the $t\bar{t}$ pair is high enough. We have also seen that we can keep the statistics high by taking advantage of the $(m_t/M_W)^2$ enhancement of longitudinally polarized W–bosons. Studying the angular distributions of these gauge bosons would aid not only in testing the top quark polarization but also in extracting the behavior of the form factors. For the purpose of these studies it would also be important to examine the angular correlations of the W^+ and W^- produced in the t and $\bar{t}$ decays.

15

4. Testing CP Violation in $t\bar{t}$ Production

The $t\bar{t}$ pair production from the standard QCD processes in (2.1) preserves CP invariance because the QCD interaction respects both C and P symmetries. One interesting question is that if the $t\bar{t}$ production violates CP invariance via some new interaction, how would we know?

If CP is violated in the production of the $t\bar{t}$, one of the consequences is to make the polarization of the t differ from that of the $\bar{t}$. Let us assume that the degree of transverse polarization $d = |P_\perp \sin \alpha|$ ($\bar{d} = |\bar{P}_\perp \sin \bar{\alpha}|$) of t ($\bar{t}$) is large enough so that we can measure it using the method described in section 2. If $d \neq \bar{d}$, then it signals a CP violation effect in the $t\bar{t}$ production process. In Appendix D we demonstrate a possibility for generating $d \neq \bar{d}$ for the $e^- e^+ \rightarrow t\bar{t}$ process.

Another method of testing CP violation is to make use of the correlation effects described in the previous section for the process

$$gg \rightarrow t\bar{t} \rightarrow W^+ b W^- \bar{b}, \tag{4.1}$$

and measure the observable

$$A = \frac{W_{up}^+ - W_{up}^- - W_{down}^+ + W_{down}^-}{2(W_{up}^+ + W_{down}^+)} \tag{4.2}$$

in the center of mass frame of $t\bar{t}$, with the Z–axis chosen along the direction of either gluon, and the t quark by definition in the first quadrant. In Eq. (4.2), $W_{up}^\pm$ ($W_{down}^\pm$) denotes the number of $W^\pm$ bosons moving toward the up (down) direction such that $\vec{p}_{W^\pm} \cdot (\vec{p}_g \times \vec{p}_t) > 0$ (< 0). $\vec{p}_t$ is the momentum of the top quark in the center of mass frame of $t\bar{t}$. By defining t (rather than $\bar{t}$) to always lie in the first quadrant, we have made a unique choice for the orientation of our coordinate axes such that the apparent ambiguity associated with having identical particles in the initial state is removed. Consequently, $\vec{p}_g$ can be either momentum of the two incoming gluons in spite of the identical particle symmetry in the initial state. If we assume that the decay of $t \rightarrow W^+ b$ is CP invariant, then $A \neq 0$ signals a CP violation in the $t\bar{t}$ production mechanism. This can be understood from the results in (B.2) that the W^+ (W^-) tends to move up if t ($\bar{t}$) is polarized upward (downward) in the rest frame of t ($\bar{t}$). Hence, if $d = \bar{d}$ then A should be zero. In practice, experimental cuts must respect CP when testing for CP violation.

We therefore conclude that at hadron colliders it is possible to test for CP violation in the production mechanism if the degree of polarization is not too small. In the SM the observable A in Eq. (4.2) average to zero. If it averaged to a non–zero value, it would demonstrate the existence of a new source of CP violation in top production.

5. Testing CP Violation in Top Quark Decays

In this section we assume the production of the $t\bar{t}$ pair is standard to simplify our argument. Consider how to test for CP violation in the decay process

$$t \to W^+ b \to l^+ \nu_l b. \qquad (5.1)$$

The obvious observable for this purpose is[20] the expectation value of the time-reversal quantity

$$\vec{\sigma} \cdot (\hat{\mathbf{p}}_b \times \hat{\mathbf{p}}_l) \qquad (5.2)$$

where $\vec{\sigma}$ is the polarization vector of t which is represented by the three–vector part of s^μ given in Eq. (C2), and $\hat{\mathbf{p}}_b$ ($\hat{\mathbf{p}}_l$) is the unit vector of the b (l^+) momentum in the rest frame of the top quark.

A detailed study of such an observable has been done in Ref. 20 for testing time reversal invariance in beta decay. Note that in Eq. (3.2), if there is a relative phase between f_1^L and f_2^R or between f_1^R and f_2^L, then CP is violated. For instance, for a left–handed bottom quark in the $m_b = 0$ limit the observable in Eq. (5.2) has a coefficient proportional to

$$Im(f_1^L f_2^{R*}). \qquad (5.3)$$

A similar functional dependence also holds for the right–handed bottom quark amplitudes with $Im(f_1^R f_2^{L*})$ in the $m_b = 0$ limit.

In the QCD process $gg \to t\bar{t}$, $P_\perp$ is at most a few percent; therefore, it will be difficult to test CP violation using such a method because the magnitude of $\vec{\sigma}$ in Eq. (5.2) is too small to be detected. One then has to study the correlation effects and measure the fraction of the longitudinal W's from the top quark decay as described in the previous sections to study these form factors. But the real reason to test CP violation at the 100 GeV scale is because new sources of CP violation whose strength increases with energy could be present, so all tests should be done.

So far we have only considered the $t\bar{t}$ pair production from the QCD processes in (2.1) and found that the degree of transverse polarization of the top quarks is only a few percent at the next to leading order. But this is not the only source for producing top quarks at hadron colliders. As pointed out by one of us in Ref. 21 the W–gluon fusion process

$$qg \to W^+ g \to t\bar{b}X \qquad (5.4)$$

can be very useful in detecting and studying top quarks. At tree level, the SM top quark produced from that process is one hundred percent longitudinally polarized.[22]

Therefore, it is much easier to study the CP properties of the top quark decay using Eq. (5.2). Besides, the non–standard piece of the $W-t-b$ couplings also contribute to the production rates of the top quark via this process.[22]

A similar process to (5.4) at the e^-e^+ colliders is the W–photon fusion process,

$$e^-e^+ \to W^+\gamma \to t\bar{b}X. \tag{5.5}$$

We note that to study CP violation effects in t decay, the top quark does not need to be transversely polarized. It is possible to observe Eq. (5.2) to test CP violation in the top quark decay process (5.1) if t is polarized transversely or longitudinally.

Before we conclude this section, we note that in Ref. 20 another time–reversal observable was studied:

$$\vec{\sigma}_l \cdot (\hat{\mathbf{p}}_b \times \hat{\mathbf{p}}_l). \tag{5.6}$$

$\vec{\sigma}_l$ is the polarization vector of the charged lepton l^+, for instance τ^+, from the top quark decay (5.1). In order to test Eq. (5.6) one has to be able to detect the polarization of the charged lepton, $e.g.$ τ^+, which remains a challenge at hadron colliders, but is possible in principle.

Summarizing, though it is expected to be difficult to test for CP violation in QCD through top quark decays, it may be that there are new sources of CP violation whose strength increases with energy. The top quark provides us with a means for testing this at the 100 GeV scale. Armed with the prerequisite polarization information, it will be possible to carry out these studies using the distribution of Eq. (5.2), and if it becomes efficient to study τ polarizations, we will have yet another means of investigating the CP properties of top decays through Eq. (5.6). In practice one has to guarantee that the experimental cuts do not bias the CP properties of the decay.

6. Polarization and Correlations in $e^-e^+ \to t\bar{t}$

We consider the process

$$e^-e^+ \to t\bar{t} \tag{6.1}$$

at the NLC (e^-e^+ collider at $\sqrt{S} = 500\,\text{GeV}$) in this section. For SM production of top quarks at the tree level, the cross section is 0.64 pb giving 6400 events per year with a $10^4\,\text{pb}^{-1}\text{yr}^{-1}$ luminosity. As in the study of the $W-t-b$ form factors,

18

the most general $V - t - \bar{t}$ coupling is

$$\Gamma^\mu_{Vtt} = ig[\gamma^\mu(F_1^L P_- + F_1^R P_+) - \frac{i\sigma^{\mu\nu}k_\nu}{m_t}(F_2^L P_- + F_2^R P_+) + k^\mu(F_3^L P_- + F_3^R P_+)], \quad (6.2)$$

where k^μ is the momentum of the gauge boson, V, and is taken by convention to be directed into the vertex. V can be the Z gauge boson or photon A, and the F's are the form factors for V. When $V = A$, F_3^L and F_3^R have to vanish due to gauge invariance (or current conservation). For a Z boson which is on–shell or coupled to massless fermions, the $F_3^{L,R}$ contributions vanish. In our case we ignore the $F_3^{L,R}$ contributions. Needless to say, $F_1^{L,R}$ and $F_2^{L,R}$ are different for $V = Z$ and $V = A$. In this section, we assume that all the new physics effects for the process (6.1) can be represented by the photon and Z mediated Feynman diagrams in Fig. 8. This assumption is certainly true when considering the QCD corrections to (6.1).

We denote the $V - e^- - e^+$ vertex as

$$\Gamma^\mu_{Vee} = ig\gamma^\mu(e_L^V P_- + e_R^V P_+),$$

where the SM values for these couplings are

$$e_L^Z = \frac{1}{\cos\theta_W}\left(-\frac{1}{2} + \sin^2\theta_W\right) \quad \text{and} \quad e_R^Z = \frac{1}{\cos\theta_W}\sin^2\theta_W \quad (6.3)$$

for $V = Z$. $e_L^A = e_R^A = Q_e$ for $V = A$, where $Q_e = -\sin\theta_W$. We focus on the diagram with the Z boson propagator because the photon propagator diagram can be treated in exactly the same way. We give the helicity amplitudes for the process (6.1) in the center of mass frame of $t\bar{t}$. The kinematics are defined so that the electron is moving along the $+Z$ direction and θ_t is the angle between the top quark and the electron. The scattering plane is defined to be the $X - Z$ plane where the X component of the top quark momentum is chosen to be always positive; we set $\phi_t = 0$.

First, we apply the Gordon decomposition to rewrite Eq. (6.2) as

$$\Gamma^\mu_{Vtt} = \frac{ig}{2}\left[\gamma^\mu(A - B\gamma^5) + \frac{t_1^\mu - t_2^\mu}{2}(C - D\gamma^5)\right], \quad (6.4)$$

where

$$A = F_1^L + F_1^R - 2(F_2^L + F_2^R) \qquad B = F_1^L - F_1^R$$
$$C = \frac{2}{m_t}(F_2^L + F_2^R) \qquad D = \frac{2}{m_t}(F_2^L - F_2^R). \qquad (6.5)$$

In Eq. (6.4), t_1^μ (t_2^μ) is the momentum of the outgoing t ($\bar{t}$). The helicity amplitudes

are denoted as $(h_{e-}, h_{e+}, h_t, h_{\bar{t}})$, where $h_{e-} = -, +$ respectively indicates a left–handed and a right–handed electron. Apart from the common factor

$$g^2 \frac{1}{S - M_Z^2} 2E,$$

with $S = 4E^2$, the nonvanishing helicity amplitudes from the diagram mediated by the Z–boson are

$$
\begin{aligned}
(-+--)_Z &= e_L \sin\theta_t [m_t A - K^2 C + EKD] \\
(-+-+)_Z &= -e_L (1 + \cos\theta_t)[EA + KB] \\
(-++-)_Z &= e_L (1 - \cos\theta_t)[EA - KB] \\
(-+++)_Z &= e_L \sin\theta_t [-m_t A + K^2 C + EKD] \\
(+---)_Z &= e_R \sin\theta_t [m_t A - K^2 C + EKD] \\
(+--+)_Z &= e_R (1 - \cos\theta_t)[EA + KB] \\
(+-+-)_Z &= -e_R (1 + \cos\theta_t)[EA - KB] \\
(+-++)_Z &= e_R \sin\theta_t [-m_t A + K^2 C + EKD].
\end{aligned}
\tag{6.6}
$$

In the above formulas, E is half the center of mass energy and $K = \sqrt{E^2 - m_t^2}$. At tree level,

$$
F_1^L = \frac{1}{\cos\theta_W}\left(\frac{1}{2} - \frac{2}{3}\sin^2\theta_W\right), \qquad F_1^R = \frac{1}{\cos\theta_W}\left(\frac{-2}{3}\sin^2\theta_W\right),
\tag{6.7}
$$

and $F_2^L = F_2^R = 0$. The nonvanishing Born helicity amplitudes from the photon propagator diagram, $(h_{e-}, h_{e+}, h_t, h_{\bar{t}})_\gamma$, can be easily obtained from the results in Eq. (6.6) by setting $e_L = e_R = Q_e$ and $F_1^L = F_1^R = Q_t$, where $Q_t = \frac{2}{3}\sin\theta_W$. The common factor in this case is

$$g^2 \frac{1}{S} 2E.$$

The helicity amplitudes for the process (6.1) are therefore obtained by summing the contributions from these two diagrams:

$$
(h_{e-}, h_{e+}, h_t, h_{\bar{t}}) = 2g^2 E\left[\frac{(h_{e-}, h_{e+}, h_t, h_{\bar{t}})_Z}{S - M_Z^2} + \frac{(h_{e-}, h_{e+}, h_t, h_{\bar{t}})_\gamma}{S}\right].
\tag{6.8}
$$

When calculating the cross section at tree level, a color factor of 3 should be included for the top quark pair production. The spin average factor $\frac{1}{2}\frac{1}{2}$ should also be included for an unpolarized $e^- e^+$. In Fig. 9, we show the polar angle θ_t distribution of the top quark in the center of mass frame of $t\bar{t}$ at NLC.

20

Using these helicity amplitudes and those listed in Appendix B for the top and anti–top quark decays, we can obtain the complete information about the W–boson kinematics including the correlations. To calculate the matrix element squared, we use the exact formula

$$|M(e^-e^+ \rightarrow t\bar{t} \rightarrow bW^+\bar{b}W^-)|^2 = \sum_{\lambda,\bar{\lambda}} \sum_{\lambda',\bar{\lambda}'} M^\dagger(e^-e^+ \rightarrow t_{\lambda'}, \bar{t}_{\bar{\lambda}'}) M(e^-e^+ \rightarrow t_\lambda, \bar{t}_{\bar{\lambda}})$$
$$\times\ M^\dagger(t_{\lambda'} \rightarrow bW^+) M(t_\lambda \rightarrow bW^+)$$
$$\times\ M^\dagger(\bar{t}_{\bar{\lambda}'} \rightarrow \bar{b}W^-) M(\bar{t}_{\bar{\lambda}} \rightarrow \bar{b}W^-)$$

$$(6.9)$$

where the summation over the helicity states of all other particles is understood.

Consider the transverse polarization of the top quark due to the QCD correction for the process $e^-e^+ \rightarrow t\bar{t}$. The degree of transverse polarization $(P_\perp \sin \alpha)$ of the top quark perpendicular to the scattering plane for this process is defined as

$$P_\perp \sin \alpha = \frac{T_\perp}{G}(\text{color factor}), \qquad (6.10)$$

where

$$G = |(+-++)|^2 + |(+-+-)|^2 + |(+--+)|^2 + |(+---)|^2$$
$$+ |(-+++)|^2 + |(-++-)|^2 + |(-+-+)|^2 + |(-+--)|^2 \qquad (6.11)$$

and

$$T_\perp = 2Im\{(+-++)^*(+--+) + (+-+-)^*(+---)$$
$$+ (-+++)^*(-+-+) + (-++-)^*(-+--)\}. \qquad (6.12)$$

The function Im selects the imaginary part of the amplitudes. The color factor in Eq. (6.10) for this process is $C_F = \frac{4}{3}$ for $SU(3)_C$. A factor of N_C comes from the Born amplitude squared when calculating G and a factor of $N_C C_F$ comes from the interference term of the Born and the one loop diagrams when calculating $T_\perp$. There is no color factor included in the definition of (6.11) and (6.12). Since we are only interested in the $O(\alpha_s)$ contribution to the transverse polarization of the top quark, the relevant form factors for the diagram with the Z–boson propagator are

$$Re(A) = 2v_t, \quad Re(B) = 2a_t, \quad Re(C) = 0, \quad Re(D) = 0,$$
$$Im(A) = v_t \frac{\alpha_s}{4\pi}(I_\infty - 6\pi\beta), \quad Im(B) = a_t \frac{\alpha_s}{4\pi}\left[I_\infty - \frac{2\pi}{\beta}(2 + \beta^2)\right],$$
$$Im(C) = v_t \frac{\alpha_s}{4\pi}\left(\frac{-8\pi m_t}{S\beta}\right), \text{ and } Im(D) = 0,$$

$$(6.13)$$

21

where

$$v_t = \frac{1}{2}(F_1^L + F_1^R), \qquad a_t = \frac{1}{2}(F_1^L - F_1^R). \tag{6.14}$$

I_∞ in Eq. (6.13), which is not infrared finite, should not appear in any physical observable. That this is true is demonstrated in Eq. (D.5). And again, applying the transformation described after Eq. (6.7) yields the relevant form factors for the photon mediated diagram. We note that the one loop QCD corrections contribute to both the photon and Z mediated diagrams in Fig. 8. Using the previous results, we show the transverse polarization $P_\perp \sin\alpha$ of the top quark produced from the process (6.1) at NLC as a function of the top quark polar angle θ_t in the center of mass frame of $t\bar{t}$ in Fig. 10(a).

We have checked that the contribution to the transverse polarization arising from a loop due to electroweak exchanges rather than gluon exchange is always less than the QCD contribution for m_t of about 140 GeV at the NLC. This includes Higgs boson exchange, whose effect is quite small.

The transverse polarization $(\overline{P}_\perp \sin\bar{\alpha})$ of the anti–top quark has the same magnitude as that of the top quark in the one loop QCD corrections for this process because QCD is a CP invariant interaction. In Appendix D, we give the explicit formula to show how it is possible to generate $P_\perp \neq \overline{P}_\perp$ from a CP violating model. The CP transformation properties of the $V - t - \bar{t}$ vertex, Eq. (6.2), is such that if $F_2^L \neq F_2^R$ then CP is violated. This implies that $Im(D) \neq 0$ would signal CP violation effects in the $t\bar{t}$ production mechanism and it will also make the transverse polarization of the t different from that of the $\bar{t}$. Obviously, a non–vanishing $Re(D)$ would also signal CP violation effects in the production of the $t\bar{t}$ pair. For instance, it will affect the correlations between the W^+ and W^- bosons from the decay of the t and $\bar{t}$.

To study the transverse polarization of the top quark at e^-e^+ colliders one can apply all the methods discussed in the previous sections for the hadron colliders. One of the methods is to study the correlations between the angles ϕ_{W^+} and ϕ_{W^-}. The exact formula, listed in Eq. (6.9), should be used to study the correlations between the W^+ and the W^- bosons. As shown in Appendix B, the effect of $P_\perp$ $(\overline{P}_\perp)$ disappears if ϕ_{W^+} (ϕ_{W^-}) is integrated from 0 to 2π.

To demonstrate the effects from both the production and decay processes, let us consider the helicity state $h_{e^-} = -$, $h_{e^+} = +$, $\lambda_{W^+} = \lambda_{W^-} = 0$. Using the helicity amplitudes for $t\bar{t}$ production, $(h_{e^-}, h_{e^+}, h_t, h_{\bar{t}})$ in Eq. (6.8), the amplitude

for this helicity state is

$$M(e^-_{h_{e^-}} e^+_{h_{e^+}} \rightarrow t\bar{t} \rightarrow bW^+_{\lambda_{W^+}} \bar{b}W^-_{\lambda_{W^-}})$$

$$= (-+--)(-0-)\overline{(-0+)} + (-+-+)(-0-)\overline{(+0+)} \quad (6.15)$$

$$+ (-+-)(+0)\overline{(-0-)} + (-++)(+0-)\overline{(+0+)},$$

where $(\pm 0-)$ and $\overline{(\pm 0+)}$ are respectively the top and anti–top decay amplitudes as explained after Eq. (3.7). If we assume that the photon propagator diagram in Fig. 8 is described by the SM tree level results and that the top quark decay form factors $f_2^L = f_1^R = 0$, then one of the interference terms generated from the square of (6.15) gives

$$\left| \frac{m_t}{M_W} f_1^L + f_2^R \right|^4 \sin^2 \theta \sin \theta_{W^+} \sin \theta_{W^-} [C_1 \cos(\phi_{W^+} + \phi_{W^-}) - C_2 \sin(\phi_{W^+} + \phi_{W^-})]$$

$$(6.16)$$

where

$$C_1 = \left[m_t Q_e Q_t + \frac{S}{S - M_Z^2} e_L Re(m_t A - K^2 C + EKD) \right]$$

$$\times \left[m_t Q_e Q_t + \frac{S}{S - M_Z^2} e_L Re(m_t A - K^2 C - EKD) \right]$$

$$+ \left(\frac{S}{S - M_Z^2} \right)^2 e_L^2 Im(m_t A - K^2 C + EKD) Im(m_t A - K^2 C - EKD),$$

$$(6.17)$$

and

$$C_2 = \left[m_t Q_e Q_t + \frac{S}{S - M_Z^2} e_L Re(m_t A - K^2 C + EKD) \right]$$

$$\times \left[\frac{S}{S - M_Z^2} e_L Im(m_t A - K^2 C - EKD) \right]$$

$$\times - \left[m_t Q_e Q_t + \frac{S}{S - M_Z^2} e_L Re(m_t A - K^2 C - EKD) \right]$$

$$\times \left[\frac{S}{S - M_Z^2} e_L Im(m_t A - K^2 C + EKD) \right].$$

$$(6.18)$$

As in Eq. (3.8), the angular correlation between the W^+ and W^- is apparent.

The longitudinal polarization of the top quark will change f_L, the fraction of the longitudinally polarized W^+ bosons which are produced from the top quark

decays. The degree of longitudinal polarization of the top quark is

$$P_\| = \frac{L}{G},$$

where G is given in Eq. (6.11) and

$$
\begin{aligned}
L = \ &|(+--++)|^2 + |(+--+-)|^2 + |(-+++)|^2 + |(-++-)|^2 \\
&- |(+---+)|^2 - |(+----)|^2 - |(-+-+)|^2 - |(-+--)|^2.
\end{aligned}
\tag{6.19}
$$

For (6.1), only the tree amplitudes are needed to compute $P_\|$ when considering the leading behavior of the helicity amplitudes. The angular dependence of $P_\|$ is shown in Fig. 10(b).

To study CP violation from the top quark decay, we again should examine the expectation value of the time–reversal observable $\vec{\sigma} \cdot (\hat{\mathbf{p}}_b \times \hat{\mathbf{p}}_l)$, as defined in Eq. (5.2). Now $\vec{\sigma}$ has both longitudinal and transverse components. Similarly, one may also examine the observable of Eq. (5.6).

In general there are two transverse components of $\vec{\sigma}$. The component we have discussed is the transverse polarization perpendicular to the scattering plane while the other one is the transverse polarization in the scattering plane and perpendicular to the motion of the top quark. The second transverse polarization is

$$P_\perp \cos\alpha = \frac{T_\|}{G} \tag{6.20}$$

where, using Re to select the real part of its argument,

$$
\begin{aligned}
T_\| = 2Re\{&(+--++)^*(+---+) + (+--+-)^*(+----) \\
&+ (-+++)^*(-+-+) + (-++-)^*(-+--)\}.
\end{aligned}
\tag{6.21}
$$

In Fig. 10(c), we show $P_\perp \cos\alpha$ as a function of θ_t for the process (6.1) at the NLC. From the amplitudes listed in Appendix A for the $gg, q\bar{q} \to t\bar{t}$ processes in the SM, we find $P_\| = 0$ and $P_\perp \cos\alpha = 0$, which is because the QCD interaction is C and P invariant. Again, new interactions that increase with energy and violate CP could emerge and should be searched for.

So far, we have only considered unpolarized $e^- e^+$ colliders. The results of Eq. (6.9), the longitudinal and transverse polarizations, and the $W^+ - W^-$ angular correlations, all can be generalized for the polarized electron and/or positron beams by introducing polarization matrices similar to the ones in Eqs. (2.3) and (2.4).

24

The matrix element squared gets modified by a weighted sum over the electron and the positron helicities,

$$\overline{|M(e^-e^+ \to t\bar{t})|}^2 = \sum_{\kappa,\bar{\kappa},\kappa',\bar{\kappa}'} M(e_\kappa^- e_{\bar{\kappa}}^+)\bar{\rho}_{\bar{\kappa}\bar{\kappa}'}M^\dagger(e_{\kappa'}^- e_{\bar{\kappa}'}^+)\rho_{\kappa'\kappa}, \qquad (6.22)$$

where the polarization matrices ρ and $\bar{\rho}$ are similar to the ones defined in Eqs. (2.3) and (2.4) except that here they refer to the polarization of the e^- and e^+ beams. The helicity amplitude $M(e_\kappa^- e_{\bar{\kappa}}^+)$ denotes the correlated amplitude (6.9) for a specific helicity state of $e_\kappa^- e_{\bar{\kappa}}^+$.

In the SM, the transverse polarization for top quarks produced in e^+e^- collisions is given by Eq. (6.10) and Eq. (6.20) while the longitudinal polarization is given by Eq. (6.19) and the lines above it. The transverse polarization is due entirely to radiative effects and is important to test. CP violation in the decay of top quarks should be zero and can be tested by finding a non–zero average value of the time reversal quantities of Eqs. (5.2) or (5.6).

7. Conclusion

We have given the helicity amplitudes for the processes $gg, q\bar{q} \to t\bar{t}$, $t \to W^+b$, $W^+ \to e^+\nu_e$, and $e^-e^+ \to t\bar{t}$, with the most general $W-t-b$ or $V-t-\bar{t}$ form factors included. Using these amplitudes, one can study the fraction of longitudinal W's from a polarized top quark decay and the correlation effects in either the production or the decay of the t and $\bar{t}$. We have proposed some methods to test the transverse polarization of the top quark because it may be sensitive to new physics. We have given the longitudinal polarization of the top quark produced in $e^+e^- \to t\bar{t}$. We also discussed how to test for CP violation effects in either the production or decay process. Using all this information, a number of new tests of the standard model can be made, many of which are sensitive to new physics at the 100 GeV scale.

In principle, the discussions presented in section 6 can be applied for the process $e^-e^+ \to \tau^-\tau^+$ to study the polarization of τ produced at LEP.

APPENDIX A

Helicity Amplitude of $gg \to t\bar{t}$ and $q\bar{q} \to t\bar{t}$

A.1 $gg \to t\bar{t}$

Because QCD is C and P invariant, only six of the sixteen amplitudes for $gg \to t\bar{t}$ are independent. Define θ_t to be the angle between the top quark t and the gluon moving along the $+Z$ direction, and $\beta = \sqrt{1 - m_t^2/E^2}$, where E is half of the c.m. energy. m_t is the mass of t. Denote the helicity amplitudes as $(h_{g1}, h_{g2}, h_t, h_{\bar{t}})$ using $-$ for a left–handed helicity state and $+$ for a right–handed helicity state. Then after suppressing the common factor

$$g_s^2 \left(\frac{C_1}{1 - \beta \cos \theta_t} + \frac{C_2}{1 + \beta \cos \theta_t} \right), \tag{A.1}$$

where the color factor $C_1^2 = C_2^2 = 16/3$ and $C_1 C_2 = C_2 C_1 = -2/3$, the nonvanishing amplitudes are

$$
\begin{aligned}
(----) &= -(++++) = -\frac{m_t}{E}(1 + \beta), \\
(--++) &= -(++--) = -\frac{m_t}{E}(1 - \beta), \\
(-+-+) &= (+--+) = -\beta \sin \theta_t (1 + \cos \theta_t), \\
(-++-) &= (+--+) = \beta \sin \theta_t (1 - \cos \theta_t), \\
(-+--) &= (+---) = -(+-++) = -(-+++) = \frac{m_t}{E} \beta \sin^2 \theta_t.
\end{aligned}
\tag{A.2}
$$

The polarization vector of the gluon which moves along the $+Z$ direction is defined to be $\epsilon_{g1}(+) = (0, -1, -i, 0)/\sqrt{2}$ for a right–handed, and $\epsilon_{g1}(-) = (0, 1, -i, 0)/\sqrt{2}$ for a left–handed. For the other gluon $\epsilon_{g2}(+) = \epsilon_{g1}(-)$ and $\epsilon_{g2}(-) = \epsilon_{g1}(+)$ in the center of mass frame of $t\bar{t}$. To obtain the averaged amplitude squared, we need to multiply by the spin and color factors

$$\frac{1}{2}\frac{1}{2}\frac{1}{8}\frac{1}{8}.$$

We note that since (A.1) is factorized out of (A.2) for all the helicity states, it will only enter the amplitude squared as

$$g_s^4 \left\{ \frac{16}{3} \left[\frac{1}{(1 - \beta \cos \theta_t)^2} + \frac{1}{(1 + \beta \cos \theta_t)^2} \right] - \frac{4}{3} \left(\frac{1}{1 - \beta^2 \cos^2 \theta_t} \right) \right\}.$$

26

A.2 $q\bar{q} \to t\bar{t}$

Let θ_t be the angle between t and q in the center of mass frame of $t\bar{t}$. In the limit $m_q = 0$ there are only 8 nonvanishing helicity amplitudes, and of those 8, only three are independent because of the C and P symmetries. Denote the helicity amplitude as $(h_q, h_{\bar{q}}, h_t, h_{\bar{t}})$. After suppressing the common factor

$$2g_s^2 \frac{1}{S} 2E, \tag{A.3}$$

the nonvanishing helicity amplitudes are

$$
\begin{aligned}
(-+--) &= (+---) = -(-+++) = -(+-++) = 2m_t \sin\theta_t, \\
(-+-+) &= (+-+-) = -2E(1+\cos\theta_t), \\
(-++-) &= (+--+) = 2E(1-\cos\theta_t).
\end{aligned}
\tag{A.4}
$$

The first 2 in (A.3) is the color factor after summing over all the initial and final state colors. To obtain the averaged amplitude squared, we need to multiply by the factor

$$\frac{1}{2}\frac{1}{2}\frac{1}{3}\frac{1}{3}.$$

APPENDIX B

Helicity Amplitude of $t \to W^+ b$ and $\bar{t} \to W^- \bar{b}$

In Eqs. (3.2) and (3.3) we have listed the most general form factors for the decay processes $t \to W^+ + b$ and $\bar{t} \to W^- + \bar{b}$. Here we use those equations to calculate the helicity amplitudes for an on-shell W–boson.

For the decay process $t \to W^+ b$, the top quark is taken to decay in its rest frame where the top quark momentum is $p_t = (m_t, 0, 0, 0)$. Spherical coordinates are used to describe the outgoing particles; θ is taken from the positive Z–axis and ϕ is taken from the positive X–axis in the $X - Y$ plane. The bottom quark and the W–boson are taken on their mass shells with the four–momenta for the bottom quark (p_b) and the W–boson (p_W) taken as

$$p_b = (E_b, -E_b \sin\theta \cos\phi, -E_b \sin\theta \sin\phi, -E_b \cos\theta),$$

$$p_W = (E_W, E_b \sin\theta \cos\phi, E_b \sin\theta \sin\phi, E_b \cos\theta),$$

where we have neglected the bottom quark mass, and

$$E_b = \frac{m_t^2 - M_W^2}{2m_t}.$$

The angles θ and ϕ refer to the direction of the W–boson.

Denote the helicity amplitudes as (h_t, λ_W, h_b) with $\lambda_W = -, +, 0$ being a left–handed, right–handed, and longitudinal W–boson. After suppressing the common factor

$$\frac{-g}{\sqrt{2}}\sqrt{2E_b m_t},$$

there are 8 nonvanishing helicity amplitudes in the rest frame of the top quark for $m_b = 0$:

$$(-\,0\,-) = \left(\frac{m_t}{M_W}f_1^L + f_2^R\right)\sin\frac{\theta}{2},$$

$$(-\,-\,-) = \sqrt{2}\left(f_1^L + \frac{m_t}{M_W}f_2^R\right)\cos\frac{\theta}{2}e^{i\phi},$$

$$(+\,0\,-) = \left(\frac{m_t}{M_W}f_1^L + f_2^R\right)\cos\frac{\theta}{2}e^{i\phi},$$

$$(+\,-\,-) = -\sqrt{2}\left(f_1^L + \frac{m_t}{M_W}f_2^R\right)\sin\frac{\theta}{2}e^{2i\phi},$$

$$(-\,0\,+) = -\left(\frac{m_t}{M_W}f_1^R + f_2^L\right)\cos\frac{\theta}{2}e^{-i\phi}, \qquad \text{(B.1)}$$

$$(-\,+\,+) = -\sqrt{2}\left(f_1^R + \frac{m_t}{M_W}f_2^L\right)\sin\frac{\theta}{2}e^{-2i\phi},$$

$$(+\,0\,+) = \left(\frac{m_t}{M_W}f_1^R + f_2^L\right)\sin\frac{\theta}{2},$$

$$(+\,+\,+) = -\sqrt{2}\left(f_1^R + \frac{m_t}{M_W}f_2^L\right)\cos\frac{\theta}{2}e^{-i\phi}.$$

To obtain the averaged amplitude squared, a spin factor $\frac{1}{2}$ should be included. We note that there is no right–handed W–boson produced with a massless left–handed b from a top quark decay. Similarly, from helicity conservation, it is not possible to have a left–handed W–boson produced with a massless right–handed b from t decay.

When we sum over the helicities of the bottom quark and perform a weighted sum over the helicities of the top quark as dictated by Eq. (2.2), the weighted amplitudes squared for various W polarizations are, apart from a common factor $(g^2 E_b m_t)$,

28

$$\overline{|M(\lambda_W = -)|^2} = \left| f_1^L + \frac{m_t}{M_W} f_2^R \right|^2 [1 - P_{\parallel} \cos\theta - P_{\perp} \sin\theta \cos(\alpha - \phi)],$$

$$\overline{|M(\lambda_W = +)|^2} = \left| f_1^R + \frac{m_t}{M_W} f_2^L \right|^2 [1 + P_{\parallel} \cos\theta + P_{\perp} \sin\theta \cos(\alpha - \phi)],$$

$$\overline{|M(\lambda_W = 0)|^2} = \frac{1}{2} \left| \frac{m_t}{M_W} f_1^L + f_2^R \right|^2 [1 + P_{\parallel} \cos\theta + P_{\perp} \sin\theta \cos(\alpha - \phi)],$$

$$+ \frac{1}{2} \left| \frac{m_t}{M_W} f_1^R + f_2^L \right|^2 [1 - P_{\parallel} \cos\theta - P_{\perp} \sin\theta \cos(\alpha - \phi)].$$

(B.2)

For QCD corrections, $\alpha = \pi/2$, and $P_{\parallel} = 0$ for a top quark polarized upward in the center of mass frame of $t\bar{t}$.

Using a parallel definition for the process $\bar{t} \to W^- \bar{b}$, we obtain the helicity amplitudes $(h_{\bar{t}}, \lambda_W, h_{\bar{b}})$, similar to the ones listed in Eq. (B.1) for the $t \to W^+ b$ process, provided we replace f_1^L by f_1^{R*}, f_1^R by f_1^{L*}, f_2^L by f_2^{R*}, and f_2^R by f_2^{L*}. The superscript $*$ means complex conjugate. Similarly, the weighted amplitude squared for various W^- polarization states can be obtained from Eq. (B.2) provided (in addition to the above mentioned substitutions) α is replaced by $\bar{\alpha}$, $P_{\parallel}$ by $\overline{P}_{\parallel}$, and $P_{\perp}$ by $\overline{P}_{\perp}$, to be consistent with the density matrix defined in Eq. (2.4). For QCD corrections, $\bar{\alpha} = -\pi/2$, and $\overline{P}_{\parallel} = 0$ for an anti-top quark polarized downward in the center of mass frame of $t\bar{t}$. Where θ and ϕ refer to the W^- boson, defined in the rest frame of $\bar{t}$.

The helicity amplitudes of the process $W^+ \to e^+ \nu_e$ are well known. After suppressing the common factor (gM_W), they are

$$(\lambda_W = -) = -e^{-i\phi_e^*} \left(\frac{1 - \cos\theta_e^*}{2} \right),$$

$$(\lambda_W = 0) = -\frac{\sin\theta_e^*}{\sqrt{2}},$$

$$(\lambda_W = +) = -e^{i\phi_e^*} \left(\frac{1 + \cos\theta_e^*}{2} \right),$$

(B.3)

where θ_e^* and ϕ_e^* refer to e^+ in the rest frame of W^+.

The helicity amplitudes (λ_W) for the decay process $W^- \to e^- \bar{\nu}_e$ can be obtained from Eq. (B.3) by replacing θ_e^* by $\pi - \theta_e^*$ and ϕ_e^* by $\pi + \phi_e^*$. In this case, θ_e^* and ϕ_e^* refer to e^- in the rest frame of W^-.

APPENDIX C

The definition of α in Eq. (2.3)

We follow the notation used in Ref. 23 to describe a polarized top quark. We denote the top quark unit momentum in the center of mass frame of $t\bar{t}$ as

$$\hat{\mathbf{p}} = (\sin\theta_t\cos\phi_t, \sin\theta_t\sin\phi_t, \cos\theta_t). \tag{C.1}$$

The polarization vector of the top quark is

$$
\begin{aligned}
s^\mu &\equiv \left(\frac{P_\|}{m_t}|\vec{\mathbf{p}}|, \vec{\sigma} \right) \\
&= P_\perp(0, \hat{\mathbf{s}}) + \frac{P_\|}{m_t}(|\vec{\mathbf{p}}|, E_t\hat{\mathbf{p}}),
\end{aligned}
\tag{C.2}
$$

where $\hat{\mathbf{s}}$ is a unit three–vector perpendicular to $\hat{\mathbf{p}}$ and E_t is the energy of top quark. The three–vector $\vec{\sigma}$ is defined in Eq. (C.2) and represents the direction in which the top quark spin is pointing. $P_\perp$ denotes the degree of transverse polarization and $P_\|$ the degree of longitudinal polarization of the top quark. Our convention is $0 \le P_\perp \le 1$, $-1 \le P_\| \le 1$, and $0 \le \sqrt{(P_\perp)^2 + (P_\|)^2} \le 1$. $\hat{\mathbf{s}}$ is chosen to be

$$
\begin{aligned}
\hat{\mathbf{s}} = (\ &\sin\psi_t\sin\phi_t + \cos\psi_t\cos\theta_t\cos\phi_t, \\
&-\sin\psi_t\cos\phi_t + \cos\psi_t\cos\theta_t\sin\phi_t, -\sin\theta_t\cos\phi_t),
\end{aligned}
\tag{C.3}
$$

so that

$$\alpha = \phi_t - \psi_t. \tag{C.4}$$

The $\bar{\alpha}$ given in Eq. (2.4) is defined similarly for an anti–top quark.

For the one loop QCD corrections to the $gg \rightarrow t\bar{t}$ process, t is polarized upward (along the $+Y$ direction) when $\theta_t < \pi/2$ in the center of rest frame of $t\bar{t}$. The scattering plane is defined to be the $X - Z$ plane so that $\phi_t = 0$. Then, $\hat{\mathbf{p}} = (\sin\theta_t, 0, \cos\theta_t)$ and $\hat{\mathbf{s}} = (0, 1, 0)$. From (C.3) we find that $\cos\psi_t = 0$ and $\sin\psi_t = -1$, therefore, $\psi_t = -\pi/2$. Hence, $\alpha = \pi/2$ for a top quark polarized upward.

APPENDIX D

A Model to Generate $d \neq \bar{d}$ in $t\bar{t}$ production

Let us consider the production process $e^- e^+ \to t\bar{t}$. To avoid finite width effects in the propagator, assume that there exists a Z' with mass close (but not equal) to twice that of the top quark mass. In addition, let us assume the coupling of this Z' to the $e^- e^+$ is the same as that in the SM. To calculate the degree of transverse polarization of the top quark, we only have to consider the diagram with the Z' boson propagator if the coupling of this Z' with $t\bar{t}$ is not particularly suppressed. The helicity amplitudes listed in Eq. (6.6) can be used with the most general form factors given in Eq. (6.5). Using Eqs. (6.10), (6.11) and (6.12), one can show that if $Im(D) \neq 0$, then $d \neq \bar{d}$, where $d = |P_\perp \sin \alpha|$ and $\bar{d} = |\overline{P}_\perp \sin \bar{\alpha}|$. Therefore, CP violation effect in the production of the $t\bar{t}$ pair is generated via a non–vanishing $Im(D)$. Obviously, if $Re(D) \neq 0$ then CP is also violated.

The degrees of transverse polarization of the top and anti–top quarks are

$$
P_\perp \sin \alpha = \frac{T_\perp}{G}(\text{color factor}) \quad \text{and} \quad \overline{P}_\perp \sin \bar{\alpha} = \frac{\overline{T}_\perp}{G}(\text{color factor}), \quad \text{(D.1)}
$$

where

$$
\begin{aligned}
G = {} & 2(e_L^2 + e_R^2)\sin^2\theta \left[m_t^2|A|^2 + E^4\beta^2(\beta^2|C|^2 + |D|^2) - 2m_t E^2\beta^2 Re(A^*C) \right] \\
& + 2(e_L^2 + e_R^2)(1 + \cos^2\theta)E^2(|A|^2 + \beta^2|B|^2) \\
& + 2(e_L^2 - e_R^2)\cos\theta[4E^2\beta Re(A^*B)], \quad \text{(D.2)}
\end{aligned}
$$

$$
\begin{aligned}
T_\perp = {} & 4(e_L^2 + e_R^2)Im(A^*C + B^*D)(E^3\beta^2 \sin\theta\cos\theta) \\
& + 4(e_L^2 - e_R^2)Im(m_t A^*B + E^2\beta^2 B^*C + E^2 A^*D)(E\beta\sin\theta), \quad \text{(D.3)}
\end{aligned}
$$

and

$$
\begin{aligned}
\overline{T}_\perp = {} & -4(e_L^2 + e_R^2)Im(A^*C - B^*D)(E^3\beta^2 \sin\theta\cos\theta) \\
& - 4(e_L^2 - e_R^2)Im(m_t A^*B + E^2\beta^2 B^*C - E^2 A^*D)(E\beta\sin\theta). \quad \text{(D.4)}
\end{aligned}
$$

In general, the color factor in Eq. (D.1) depends on the group structure of the theory. For instance, in considering the one loop QCD corrections, this color factor is $C_F = \frac{N^2-1}{2N} = \frac{4}{3}$ for the $SU(N = 3)_C$ group.

With the one loop QCD corrections, (6.13) and (6.14), we get

$$
P_\perp \sin \alpha = \frac{4\alpha_s}{3}\frac{m_t}{2E}\frac{-\beta\sin\theta[v_t^2(e_L^2 + e_R^2)\cos\theta + a_t v_t(e_L^2 - e_R^2)(\frac{2}{\beta} - 2\beta)]}{(e_L^2 + e_R^2)[v_t^2(2 - \beta^2\sin^2\theta) + a_t^2\beta^2] + 4a_t v_t(e_L^2 - e_R^2)\beta\cos\theta}
$$

$$\text{(D.5)}$$

where e_L and e_R are given in (6.3). The color factor is $C_F = 4/3$ for $SU(3)_C$. Note that because $Im(D) = 0$ for QCD, the degree of transverse polarization of

31

the anti–top quark has the same magnitude as that of the top quark in the one loop QCD corrections for this process, but new interactions could lead to $d \neq \bar{d}$.

The same argument also holds for the process $q\bar{q} \to t\bar{t}$ via the Z' intermediate state. At LEP, the transverse polarization of $\tau^- \tau^+$ pair produced near the Z^0 due to the QED corrections can also be found using the result (D.5) provided that the factor $4\alpha_s/3$ is replaced by $\alpha_{e.m.}$, and m_t, v_t, a_t by m_τ, v_τ, a_τ.

REFERENCES

1. G.S. Abrams *et al.* (MARK II Collaboration), Phys. Rev. Lett. **63** (1989) 2447; D. Decamp *et al.* (ALEPH Collaboration), Phys. Lett. **B231** (1989) 519; Phys. Lett. **B235** (1990) 399; B. Adena *et al.* (L3 Collaboration), Phys. Lett. **B231** (1989) 509; P. Aarnio *et al.* (DELPHI Collaboration), Phys. Lett. **B231** (1989) 539; M.Z. Akrawy *et al.* (OPAL Collaboration), Phys. Lett. **B231** (1989) 530.

2. F. Abe *et al.* (CDF Collaboration), Phys. Rev. Lett. **64** (1990) 147.

3. G.L. Kane, J. Pumplin and W. Repko, Phys. Rev. Lett. **41** (1978) 1689; A. Devoto, G.L. Kane, J. Pumplin and W. Repko, Phys. Rev. Lett. **43** (1979) 1062; Phys. Rev. Lett. **43** (1979) 1540; A. Devoto, G.L. Kane, J. Pumplin and W. Repko, Phys. Lett. **90B** (1980) 436.

4. J. Liu and Y.-P. Yao, University of Michigan preprint UM-TH-90-09; C.S. Li, R.J. Oakes and T.C. Yuan, preprint NUHEP–TH–90–27; M. Jezabek and J.H. Kuhn, Nucl. Phys. **B314** (1989) 1; *ibid* **B320** (1989) 20.

5. R.D. Peccei and X. Zhang Nucl. Phys. **B337** (1990) 269.

6. W.G.D. Dharmaratna and G.R. Goldstein, Phys. Rev. **D41** (1990) 1731.

7. I.I.Y. Bigi, Yu L. Dokshitzer, V.A. Khoze, J.H. Kuhn, and P. Zerwas, Phys. Lett. **181B** (1986) 157; L.H. Orr and J.L. Rosner, Phys. Lett. **246B** (1990) 221; **248B** (1990) 474(E).

8. G. R. Farrar and F. Neri, Phys. Lett. **B130** (1983) 109; G. A. Ladinsky, Phys. Rev. **D39** (1989) 2515.

9. K. Hagiwara and D. Zeppenfeld, Nucl. Phys. **B274** (1986) 1.

10. J. Gunion and Z. Kunszt, Phys. Lett. **161B** (1985) 333.

11. P. Nason, S. Dawson and R.K. Ellis, Nucl. Phys. **B303** (1988) 607; **B327** (1989) 49.

12. W. Beenakker, H. Kuijf, W.L. van Neerven and J. Smith, Phys. Rev. **D40** (1989) 54; W. Beenakker, W.L. van Neerven, R. Meng, G.A. Schuler and J. Smith, DESY 90-064 (1990); R. Meng, G.A. Schuler, J. Smith and W.L. van Neerven, Nucl. Phys. **B339** (1990) 325.

13. D. Kuebel, M. Pundurs, C.-P. Yuan, E.L. Berger and F.E. Paige, Phys. Rev. **D43** (1991) 767.

14. J.G. Morfin and Wu-Ki Tung, Fermilab–Pub–90/74, IIT–PHY–90/11.

15. A. Denner and T. Sack, Leiden Print-91-0031 (1991); G. Eilam, R.R. Mendel, R. Migneron and A. Soni, Technion-PH-90-37 (1991); B.A. Irwin, B. Margolis, and H.D. Trottier, Phys. Lett. **B256** (1991) 533.

16. C.A. Nelson, Phys. Rev. **D41** (1990) 2805; SUNY-BING-8/15/89 (E).

17. R.P. Kauffman and C.-P. Yuan, Phys. Rev. **D42** (1990) 956; G.A. Ladinsky and C.-P. Yuan, Phys. Rev. **D43** (1991) 789.

18. V. Barger, J. Ohnemus and R.J.N. Phillips, Int. Jour. of Mod. Phys. **A4** (1989) 617.

19. G.L. Kane, G. Vidal and C.-P. Yuan, Phys. Rev. **D39** (1990) 2617.

20. J.D. Jackson, S.B. Treiman and H.W. Wyld, Jr., Phys. Rev. **106** (1957) 517; R.B. Curtis and R.R. Lewis, Phys. Rev. **107** (1957) 543.

21. C.-P. Yuan, Phys. Rev. **D41** (1990) 42.

22. J.C. Collins and C.-P. Yuan, in preparation.

23. K. Hagiwara and D. Zeppenfeld, Nucl. Phys. **B274** (1986) 1; H.A. Olsen, P.Osland and I. Overbo, Nucl. Phys. **B171** (1980) 209; T. Sjostrand, Comput. Phys. Comm. **28** (1983) 229.
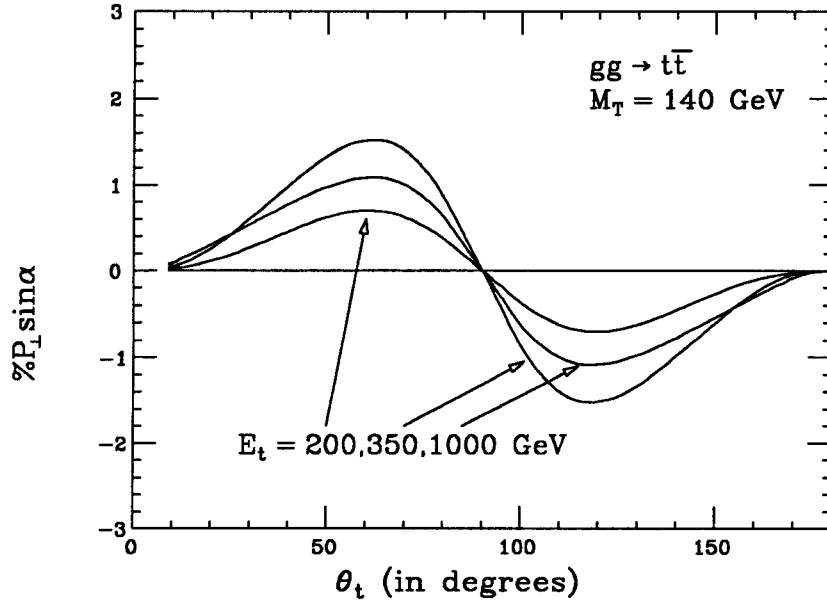
Fig. 1. The degree of transverse polarization of the top as a function of its polar angle θ_t for various top quark energies E_t in the center of mass frame of a $t\bar{t}$ pair produced from the gluon fusion process.
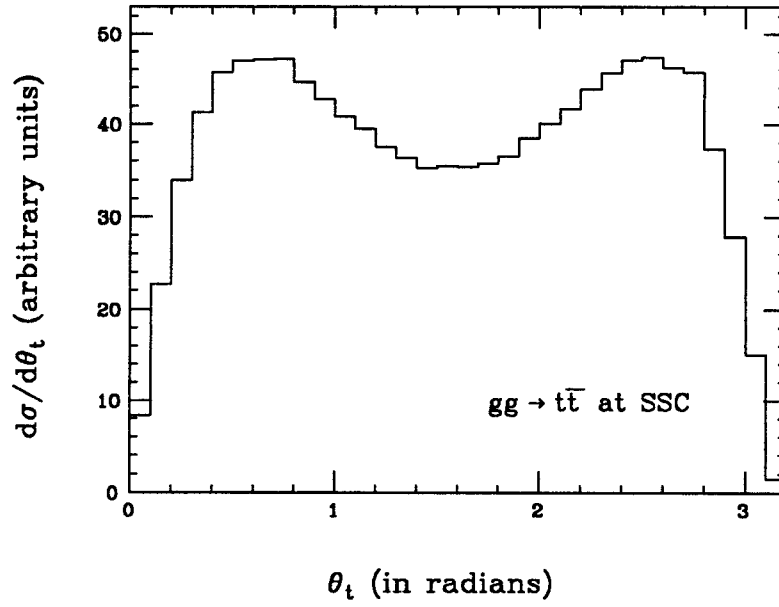

Fig. 2. θ_t distribution for a 140 GeV top quark produced via the gluon fusion process at the SSC.
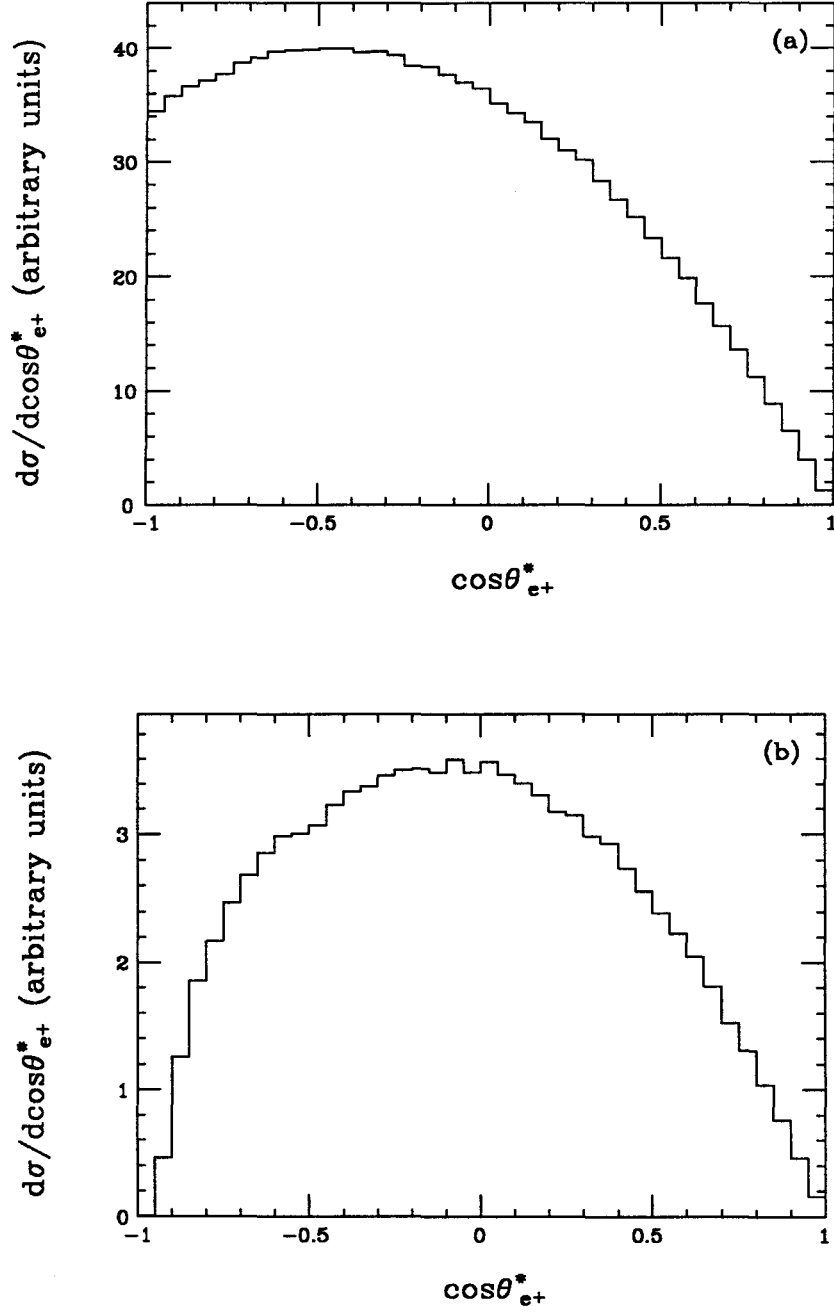
Fig. 3. $\cos\theta^*_{e+}$ distribution for an unpolarized 140 GeV SM top quark. The vertical scale is arbitrary. (a) No kinematic cuts are made. (b) With the cuts (2.6).
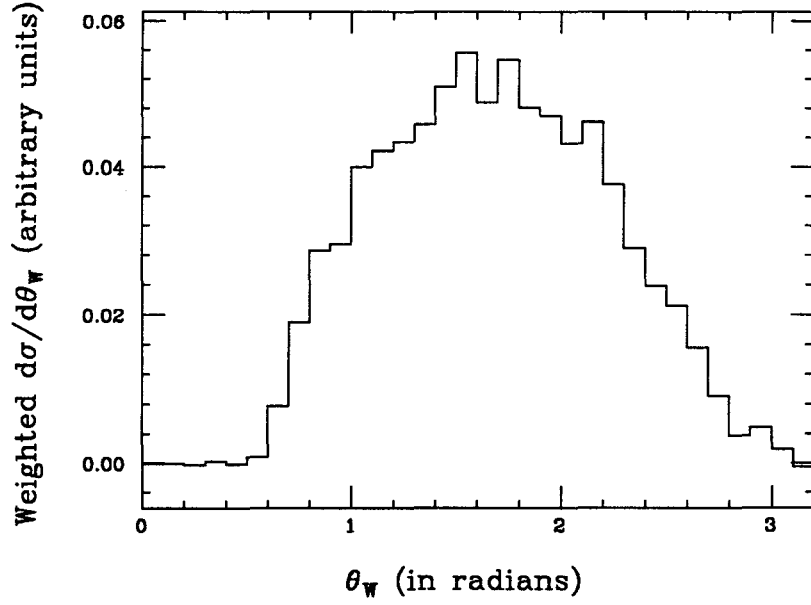
Fig. 4. The weighted θ_W distribution after imposing (2.10) and the cuts (2.6) and (2.11) for a completely transversely polarized 140 GeV SM top quark produced from the gluon fusion process at the SSC. The vertical scale is arbitrary.
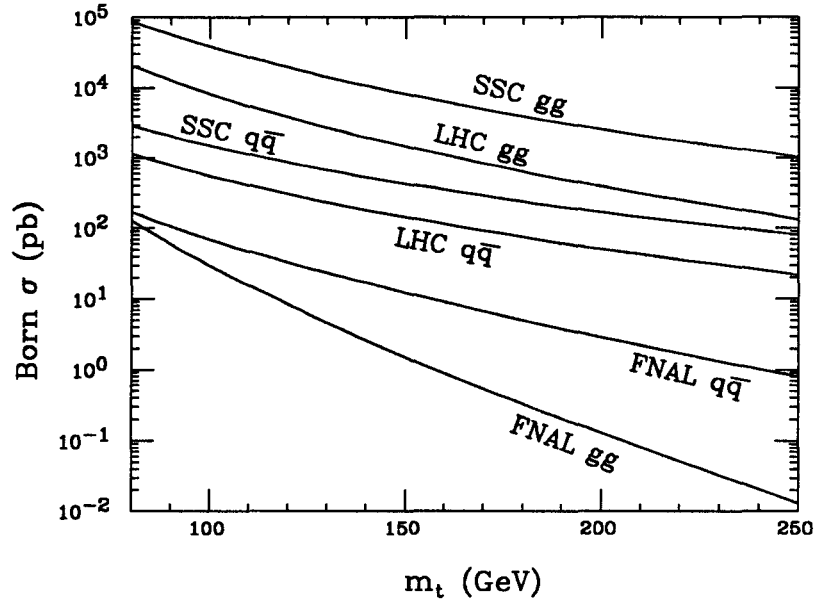

Fig. 5. The Born cross sections for both the gluon–gluon fusion and quark–antiquark annihilation processes in (2.1) at the SSC, LHC and Tevatron. No kinematic cuts are made.
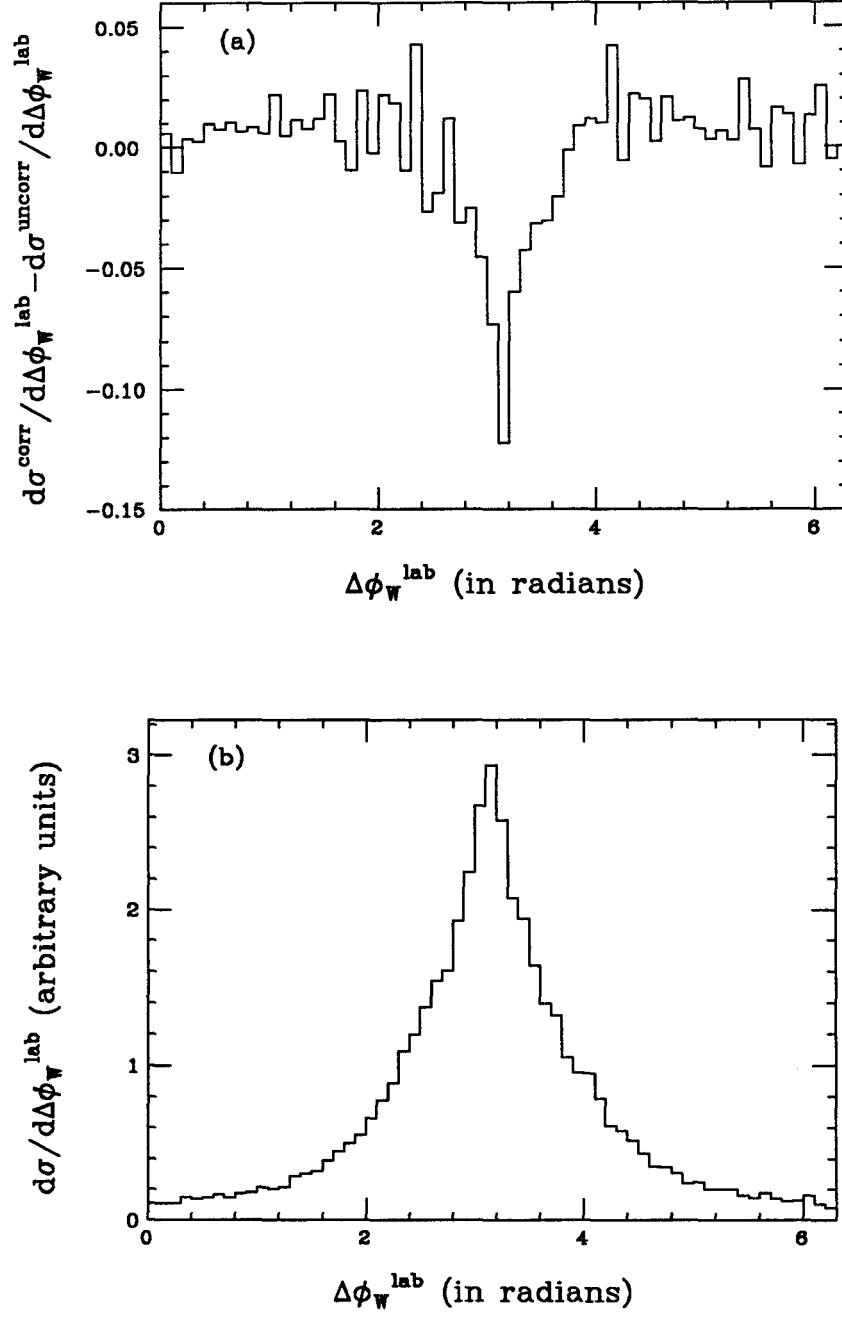
(a)

0.05

0.00

−0.05

−0.10

−0.15

$d\sigma^{corr}/d\Delta\phi_W^{lab} - d\sigma^{uncorr}/d\Delta\phi_W^{lab}$

0   2   4   6

$\Delta\phi_W^{lab}$ (in radians)

(b)

3

2

1

0

$d\sigma/d\Delta\phi_W^{lab}$ (arbitrary units)

0   2   4   6

$\Delta\phi_W^{lab}$ (in radians)

Fig. 6. (a) The difference between using Eq. (2.5) and Eq. (2.2) in the $\Delta\phi_W^{lab}$ distribution for an unpolarized 140 GeV SM $t\bar{t}$ pair produced from the gluon fusion process at the SSC. (b) The $\Delta\phi_W^{lab}$ distribution using Eq. (2.5).
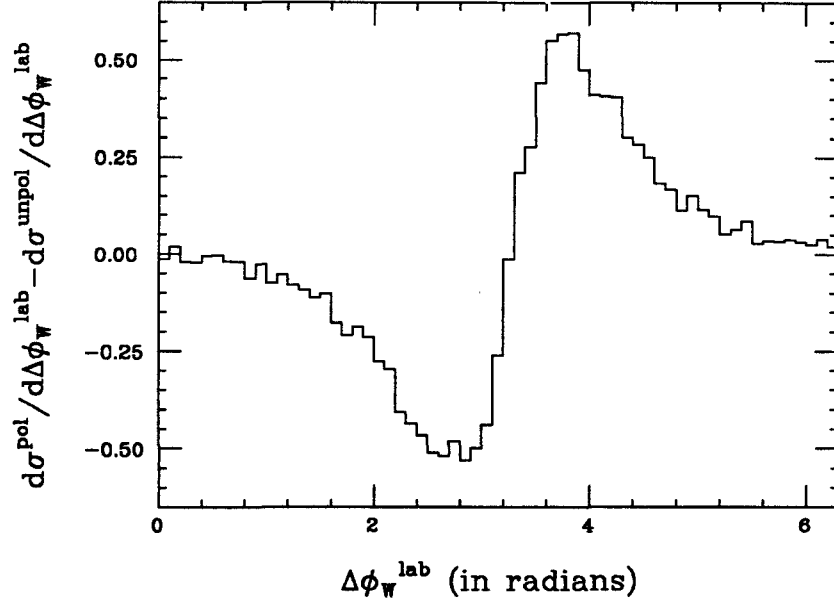
Fig. 7. The difference between a completely transversely polarized t (and $\bar{t}$) and an unpolarized t (and $\bar{t}$) using Eq. (2.2) for the $\Delta\phi_W^{lab}$ distribution for a 140 GeV SM $t\bar{t}$ pair produced from the gluon fusion process at the SSC.
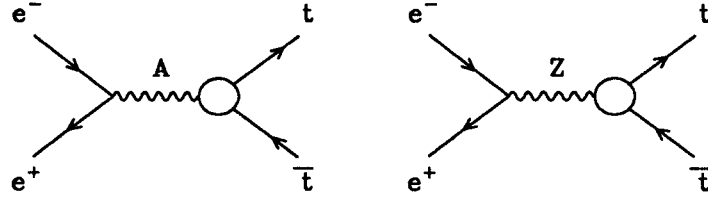

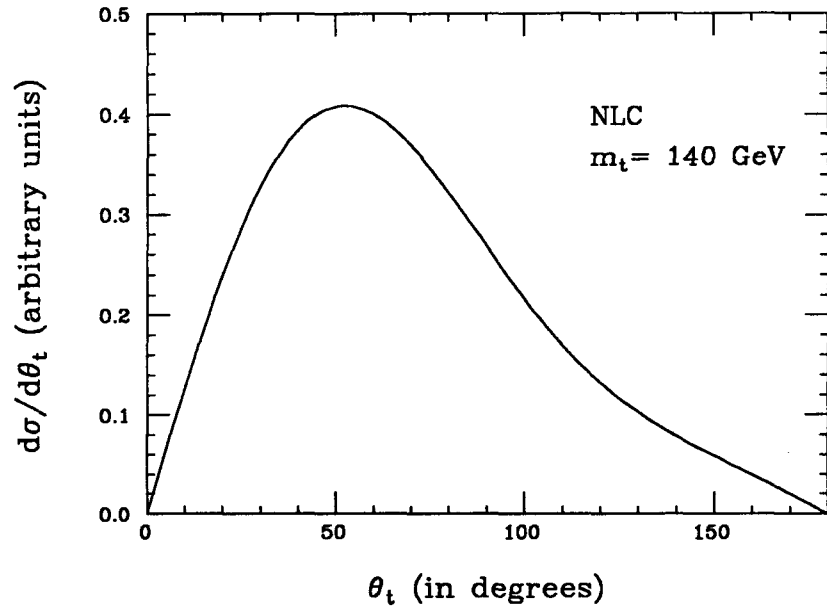Fig. 8. Feynman diagrams for the process $e^- e^+ \rightarrow t\bar{t}$.

Fig. 9. θ_t distribution of the top quark in the center of mass frame of $t\bar{t}$ at NLC. The vertical scale is arbitrary.
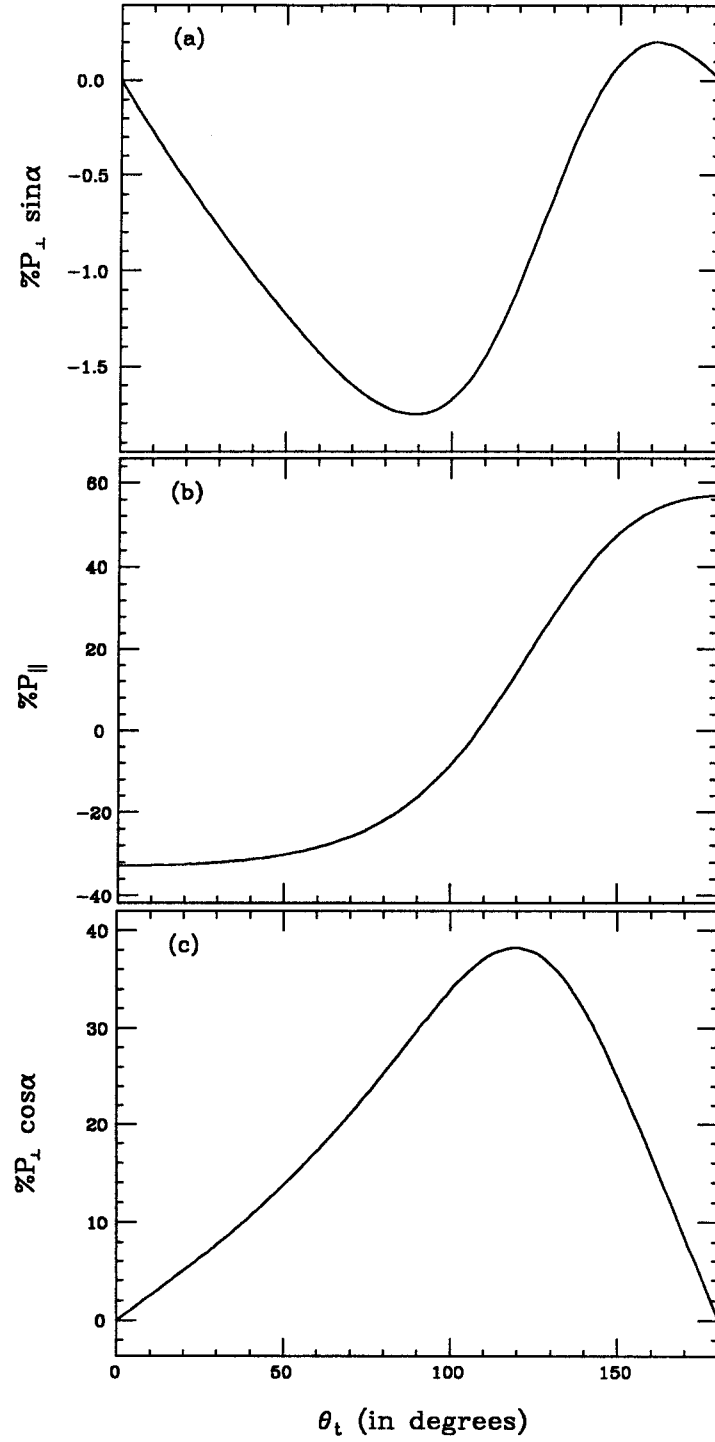
Fig. 10. (a) $P_\perp \sin\alpha$ of the top quark produced from the process (6.1) at NLC as a function of the top quark polar angle θ_t in the center of mass frame of $t\bar{t}$. (b) Same for $P_{||}$. (c) Same for $P_\perp \cos\alpha$.

40